WATSON, CHARLES, Ph.D. Analysis of Urban Heat Island Climates along the I-85/I-40 Corridor in Central North Carolina (2012).
Directed by Drs. Roy Stine & Gerald Lennartson. 77 pgs.

Land surface temperature is a significant parameter for identifying micro-climatic changes and their spatial distributions relative to the urban environment. This paper examined and identified the urban heat islands and their spatial and temporal variability along the I-85/I-40 corridor in central North Carolina between 1990 and 2002. More specifically, the study focused on: (1) understanding the behavior of the spectral and thermal signatures of various land cover and land use types and their relationships with UHI development, and (2) applying digital remote sensing techniques to observe and measure the temporal and spatial variability of these surface heat islands. An assemblage of remotely sensed imagery (Landsat data), land surface temperature data, land cover and land use classifications, vegetation indices, and archived weather data was used to create maps, charts and statistical models to indicate and display the magnitude and spatial extent of these thermal climates. The data revealed that urbanization in the I-85/I-40 corridor region increased significantly between 1990 and 2002. Quantitative results from the satellite imagery also indicated that differences in land cover/ land use types, anthropogenic heat sources, and land surface temperature variability likely contributed to a temperature rise in the corridor study area thus thermal climate development.

ANALYSIS OF URBAN HEAT ISLAND CLIMATES ALONG THE I-85/I-40 CORRIDOR IN CENTRAL NORTH CAROLINA

by

Charles Watson

A Dissertation Submitted to
the Faculty of the Graduate School at the
University of North Carolina at Greensboro
in Partial Fulfillment
of the Requirements for the Degree of
Doctor of Philosophy

Greensboro
2012

Approved by

Dr. Roy Stine_____
Committee Co-Chair

Dr. Gerald J. Lennartson_____
Committee Co-Chair

This dissertation is dedicated first and foremost to Almighty God whose guidance and direction would not have made this paper possible. Also, my loving and faithful wife, Brenda Rene Watson, who continued to give me love, encouragement and support which made this research a reality.

APPROVAL PAGE

This dissertation has been approved by the following committee of the Faculty of The Graduate School at the University of North Carolina at Greensboro.

Committee Co- Chairs _____
Dr. Roy Stine

_____
Dr. Gerald Lennartson

Committee Members _____
Dr. Elisabeth Nelson

_____
Dr. William Markham

_____
Date of Acceptance by Committee

_____
Date of Final Oral Examination

ACKNOWLEDGEMENTS

I am glad to acknowledge the voluntary and professional assistance from many people and constituents. First and foremost, my advisor and mentor, **Dr. Gerald Lennartson.** His vision, encouragement, support, and love for my work made this research not only a reality, but a delightful pleasure and enjoyment.

My committee members, **Dr. Roy Stine, Dr. Elisabeth Nelson, and Dr. William Markham** provided valuable guidance through all the phases of research. I would sincerely like to thank **Dr. John Hidore** who believed in me and made my academic dreams come true. I also want to thank **Dr. Jeff Patton** and the entire **Department of Geography at UNC-Greensboro** faculty and staff. Each of them played a role in developing me into a geographer/climatologist and a much improved human being.

Ms. Mary Hall-Brown (Beebee) for her sensational guidance and encouragement throughout all the phases of this research. She was like a 5th committee member who had a genuine interest in my work and supplied significant information that kept this research on track. **Dr. Prasad Pathak** for his technical brilliance on some of the various stages of the imaging process.

I also own my indebtness to **Dr. Augustin Misago, Mr. Alvin Jones**, and my two loving daughters, **Latoya Rene Gladney and Sherelle Lynette Green.**

TABLE OF CONTENTS

Page

LIST OF TABLES

Page

LIST OF FIGURES

Page

CHAPTER I

INTRODUCTION

1.0. Urban Heat Islands

Understanding the interactions among urban land cover types, atmospheric conditions, and surface temperatures is essential to the study of urban climatology. Modifications of land cover in urban areas influences these interactions, which are governed by the distribution of surface heat fluxes, causing surface temperatures to rise. These surface modifications, due to urbanization, generally lead to a modified thermal climate that is warmer than the surrounding countryside, particularly after sunset. The process of urbanization can increase local temperatures, whereas temperatures in less built-up suburban/rural areas generally will remain constant (Rosenweig et al. 2005). This climatic phenomenon is known as the urban heat island, or UHI (Landsberg, 1981).

The UHI results from an altered radiation and energy budget in the urban environment. Luke Howard (1833) was the first to detect the UHI during a study of London's urban climate. Oke (1982) compiled a list of the commonly hypothesized causes of the UHI. They include: (1) increased absorption of short wave radiation because of multiple reflection; (2) anthropogenic heat sources; (3) decreased outgoing long wave radiation due to decreased sky view (air pollution); (4) decreased radiational cooling; (5) increased sensible heat storage because of higher thermal admittance of building materials; (6) decreased evapotranspiration due to construction material; and

(7) decreased total turbulent heat fluxes from wind speed reduction in the city. Oke (1982) also identified several characteristics that affect the UHI. These include decreasing UHI with increasing wind speed and cloud cover; increasing UHI with city population and size; and stronger UHI effects during summer to late fall seasons. UHIs have caused changes in urban precipitation and temperature that are at least similar to, if not greater than, those predicted by global change models (Changnon, 1992). Elevated temperatures associated with UHIs increase the risk of climatic and biophysical hazards in urban environments, including heat stress, anxiety, and heightened acute and chronic response to air pollutants (Rosenweig et al. 2005).

Urban heat islands also have a significant impact on energy demand, human health, and environmental conditions (Stathopoulou & Cartalis, 2004). The intensity of an UHI (UHII) can be quantified by determining the maximum difference between urban minimum temperature and the rural minimum temperature in consideration with the urban characteristics of the city (size, population, physical layout, topography, and atmospheric conditions) (Oke, 1991). Maps of UHIs depicting urban locations that produce “hot spots” within the city can provide useful information to urban planners regarding new measures that may reduce the undesirable impact on the urban thermal environment and at the same time contribute to the microclimatic rehabilitation of a city (Stathopoulou & Cartalis, 2004).

The UHI effect has been the subject of numerous studies in recent decades and is present in many cities, small or large, around the world (Streutker, 2003). Previous studies of UHI relied on either ground-based observations taken from fixed weather

instrumentations or automobile traverses. Data collected at weather stations in cities, however, often misrepresent urban weather conditions because most studies are calibrated to forecast synoptic climatic parameters at places where the elements of weather are not disturbed by urban morphology and human activities (Lee, 1992). Measurements from automobile traverses are made at sunroof level, which may not necessarily be representative of the surface where most energy exchanges are occurring (Henry, 1989; Lee, 1992).

With the advent of thermal remote sensing technology, observations of UHI's have become possible using satellite and aircraft platforms. This has provided new direction for the observations of UHIs and the study of their effects through the combination of thermal remote sensing and urban micrometeorology (Voogt, 2003). Satellite borne instrumentation provides quantitative physical data at high spatial (120m, 60m, 30m, etc.) and low temporal (twice daily image collection) resolutions. Visible and near infrared remote sensing systems have been extensively used to classify city growth, study changes in population, vegetation indices, and examine land use/land cover changes (Doussert, 2002). These remote sensing systems also are gradually replacing traditional land cover monitoring methods that depend on field surveys (Yaboub, 2003).

The idea of combining remote sensing technologies and archived minimum temperature data has been employed in several UHI studies conducted in various cities around the world, but it has yet to be applied to the I-85/I-40 corridor area of central North Carolina. It will be useful to conduct such a study in this geographic area because it is important to learn if the temperatures in the corridor area are increasing, perhaps as a

result of the UHI effect. An understanding of the spatial and temporal characteristics of the UHI effect along the I-85/I-40 corridor has to be achieved before mitigation efforts can be applied to reduce the expansion of the UHI in the I-85/I-40 corridor in central North Carolina. Combining remote sensing technologies with archived minimum temperature data will be the approach that this study employs to examine and analyze the spatial and temporal characteristics of the UHI in the I-85/I-40 corridor area of central North Carolina.

2.0. Objectives

This research examined the urban heat islands found in the corridor area of central North Carolina, analyzing the temporal and spatial changes on the UHI along the corridor from 1990 to 2002. Additionally, the relationships between land surface temperatures (LSTs) and vegetation (via the Normalized Difference Vegetation Index, or NDVI) was used to analyze the UHI in the corridor . This was accomplished by: (1) displaying unsupervised classifications of the corridor cities and surrounding area from selected Landsat satellite images chosen for this analysis to observe the spectral signatures from various urban/rural land cover types; (2) displaying NDVI maps indicating vegetation and non-vegetation density and assigning spectral emissivity values and their relationship with UHI development along the I-85/I-40 corridor during both the 1990 and 2000 time intervals; (3) displaying land surface temperature maps created from thermal band 6 data showing the remotely-sensed temperatures relative to the land cover/land use thermal signatures of the corridor area; (4) displaying the relationships uncovered between LSTs

and NDVIs of the region ; and (5) validating Lee's (1992) concepts that remote sensing methods are useful and effective in analytical interpretations of temperature data.

This study examined the nature of the spectral and thermal signatures from the different land cover and land use types within urban and rural areas during early and late morning hours and explored their roles in UHI development, growth, and variability in the corridor area. These spectral/thermal signatures from different land cover/land use types revealed patterns of UHI development because the radiative transfer varied dramatically over space due to urban land cover diversity and its respective physical properties (Gluch & Quattrochi, 2006). As the cities in the I-85/I-40 corridor area continue to expand and grow, more commercial/industrial/residential development along with road networks will surely follow. The spatial locations of buildings and pavements within an urban landscape can also affect the spatial extent of the UHI (Lo & Quattrochi, 1996). This means that urban planners and city government officials need innovative ways to promote development and placement of construction materials to encourage healthy and sustainable growth for the urban communities in the corridor area in order to manage the growth of UHI's. The use of remote sensing imagery will become progressively more important for researchers and decision makers to understand this urban/rural energy transfer, which will contribute to controlling urban development in the corridor area (Hung, Uchihama, 2005).

This study should not only prompt comparative studies of UHI between cities with different climatic and socio-economic settings, but also contribute new information and knowledge to academia, local, state, and federal affiliates, developers, environmental

interest groups, and other stake holders for better understanding of how to mitigate these thermal climates.

CHAPTER II

LITERATURE REVIEW

1.0. First UHI Studies Using Remote Sensing

Satellite derived surface temperatures, especially those obtained from the Landsat Thematic Mapper (TM) and Landsat Enhanced TM (ETM) sensors on board the Landsat satellites of the National Aeronautics and Space Association (NASA) have been utilized for several urban climate analyses such as UHI spatial variability, UHI development, and urban surface temperature acquisition. The first known surface UHI observation from satellite-derived sensors was reported by Rao (1972). Rao utilized thermal IR data acquired by the Improved TIROS Operational Satellite (ITOS-1) to examine surface temperature patterns for the cities along the mid-Atlantic coast. Rao found that the surface temperature patterns varied from city to city and that the warmest areas were within the urban core areas. Since then, a variety of sensor platform combinations (aircraft and satellite) have been used to make remote observations of the UHI or of urban surface temperatures that contribute to UHI development (Voogt & Oke, 2000).

According to Roth (1989), the heterogeneity of the urban environment was difficult to interpret, and the temperatures that were extracted from the AVHRR and Landsat data introduced bias. However, a study led by Henry (1989) emphasized how remote sensing techniques can cover the urban canopy as a whole and have the capability of repeated synoptic coverage. Furthermore, Lee (1992) stated that remote sensing

methods can overcome many of the problems of other techniques and several researchers suggest that the data derived from their methods are the most viable for UHI studies.

Some of the sensors that have been employed in urban studies are (1) Landsat TM/ETM, (2) Advanced Spaceborne Thermal Emission Radiometer (ASTER), (3) Advanced Thermal and Land Applications Sensor (ATLAS), (4) Moderate Resolution Imaging Spectroradiometer (MODIS-Terra) and the widely used (5) Advanced Very High Resolution Radiometer (AVHRR). Many of the early UHI studies that utilized remote sensing imagery were conducted in several European and Asian cities (London, Berlin, Rome, Tokyo, etc.). During the late 1980's and early 1990's, an increase in UHI studies using remote sensing imagery were being performed at selected large US cities (St. Louis-1987; Indianapolis-1990; Washington, D.C.-1992; etc.).

The UHI studies referenced in this research acquired and analyzed their temperature datasets from the Landsat TM/ETM and AVHRR sensors. These studies will be summarized in two sections: The first section will examine urban heat island studies that focus on the growth and change of the thermal climate and the second section will examine the studies that emphasize the use of correlation and linear regression techniques to see if there are any relationships between the temperature datasets.

2.0. Growth and Change of Urban Heat Islands

Lee's (1992) results from a Seoul UHI study indicated that the areal magnitude of the thermal climate had expanded dramatically over a three-year period. Seoul's heat islands

especially spread out from Seoul to rural areas to a large degree. The temperatures of Seoul's satellite cities increased during this period dramatically while solar radiation decreased relative to urbanization. Lee's results show that the expansion of heat islands was associated not only with urban structures but also with such socioeconomic factors as the increase of industries, intensification of urban land use, and population growth. Lee created isothermic maps based on the values of brightness temperatures derived from AVHRR (channel 4) thermal data to assess the characteristics of the UHI. The change and growth of Seoul's UHI was very pronounced based on the patterns of brightness temperature values.

Streuker's (2003) study of Houston's urban heat island revealed that the growth of the UHI, both in magnitude and spatial extent (using Gaussian interpolation), was relative to the increase in Houston's population. The increases in spatial extent resulted in a change in overall area from 38% to 88%. Houston's population grew about 20% between 1990 and 2000 and one manifestation of this considerable growth is based on this spatial extent of the heat island signature (Streuker, 2003). The study period for Houston was from 1987 to 1999; it also revealed that the mean nighttime surface temperature heat island of Houston increased. Streuker noted that while the spatial extent of the UHI is related to total urban population, the magnitude of the UHI may be more closely related to urban population density than overall population.

Stathopoulou and Cartalis (2006) observed the UHI's in the coastal cities of Greece using Landsat ETM thermal data in conjunction with the CORINE land cover application (a geographic land cover/land use database for a pan-European region). Their

results indicated the presence of UHI's with the highest temperatures along the coastal zone of the harbor cities due to the density of urban environment and intense pattern of human activity. The city of Athens showed that the central business district was 3.3 degrees C warmer than rural areas, whereas suburban areas are about 2.3 degrees C warmer than rural areas. Increased proportion of impervious surfaces, local structure development, airport runway improvements, and overall growth of the city have contributed to the various "hot spots" that are located throughout the city.

3.0. Statistical Analyses of Urban Heat Islands

Regression analyses are statistical tools that have been used extensively in UHI studies. These statistics are useful in showing the significance of the relationships between different variables, in this case different temperature and NDVI datasets. The second part of this literature review will focus on studies pertaining to the application of regression techniques for comparative analysis of temperature and NDVI datasets.

According to Lee (1992), linear and multiple regression techniques can be used to perform several statistical tasks on temperature datasets. Lee utilized linear and multiple regression to compare satellite derived brightness temperatures with air and ground surface temperatures to determine whether there was any relationship among the parameters in question. Based on the thermal infrared images of Seoul taken in 1986 and 1989, urban areas and heat islands in the Seoul metropolitan area expanded dramatically. Regressing archived land surface temperatures on the brightness temperatures explained 72% of the variance in this study, making it a useful tool for assessing changing air

temperature fields in cities. Lee emphasized how the equation verifies that one can estimate and predict ground surface temperatures based on the brightness temperatures.

The approach that Gallo and McNab (1993) utilized was very similar to Lee's method but with different algorithms for analysis. Gallo and McNab (1993) used the vegetation index, satellite derived surface temperatures, and air temperatures for their study while performing multiple regression on these parameters. Urban/rural differences for the vegetation index and the remotely sensed land surface temperatures were computed and compared to observed urban/rural differences in minimum air temperatures (UHI intensity). The temporal range of the analysis was from June 28 to July 4, 1991 and provided an evaluation of data from single dates compared with data from weekly composites along with the vegetation index. The vegetation index and surface minimum temperatures were sampled from these days (July 1, 2, & 3, 1991--clear conditions) and the relationships were examined for each day. The vegetation index was obtained from channels 1 (.62um--.91um.) and 2 (.91um—3.74um) of the AVHRR sensor, both of which were used in various vegetation cover analyses.

These authors found that the satellite-derived normalized difference vegetation index data (NDVI), sampled over urban and rural areas composed of a variety of land surface environments, were linearly related to the differences in observed urban and rural minimum temperatures when linear regression was performed. The purpose of these comparisons was to evaluate the use of satellite imagery to assess the influence of the urban environment on the UHI effect. The difference in the NDVI between urban and

rural regions appears to be an indicator of the difference in surface properties between the two environments that are responsible for the UHI effect.

A slightly different statistical approach was used in the Florio et al. (2004) study, which addressed whether combining several different statistical models with satellite data information improved the performance in surface air temperature prediction. Three spatially dependent (kriging) models were examined along with their non-spatial counterparts (linear and multiple regression). Both models predicted temperature very accurately; however, the kriging models had lower errors (average of 0.9 degrees C) than the regression models (—average of 1.4 degrees C). The purpose of the Florio et al. (2004) study was to (1) evaluate the predictive performance of the statistical approaches that use only the ground level data and no satellite data and (2) introduce models that utilize the satellite data along with ground level data and evaluate their predictive performance. Their results provided an assessment of surface air temperature predictive performance of various statistical models, with and without satellite data, over different imaging conditions. Generally, the integration of satellite temperature data and ground temperature data into one statistical model showed promise as an approach for increasing the precision of air temperature measurements at the surface and can be useful in land surface temperature modeling.

A pixel-by-pixel correlation analysis of Indianapolis, Indiana was conducted by Weng and Lu (2007) in which they computed Pearson's correlation coefficients between LST's, green vegetation, and impervious surfaces. Three dates of Landsat TM imagery acquired in 1991, 1995, and 2000 were utilized to document the morphological changes

in impervious surfaces and vegetation cover and analyzed the relationships between these changes and those that occurred in land surface temperatures. Their results indicated that all land use- land cover types and LST values were negatively correlated with the green vegetation fraction values, but were positively correlated with impervious surface fraction values. Temperature increases occurred in areas where vegetation cover was lost due to imperviousness from 1991 to 1995 and from 1995 to 2000. They also concluded that the spatial arrangement and areal extent of different land cover types was a significant factor contributing to the variations of spectral radiance in LST's and the spatial patterns and development of the UHI.

CHAPTER III

METHODS

1.0. Study Area

The I-85/I-40 corridor between Kernersville and Burlington (Figure 1), which contains the Piedmont Triad region, has been selected as the study area because of its rapid urbanization in the past 20 years. The area is an oblong-shaped region approximately 30,000 square km in which Reidsville is the northernmost point and Asheboro is the southernmost point. The rapid acceleration of urbanization and commericialization of the area has been recognized along with the developing warm urban climate.

The study area is located in the Piedmont physiographic division of the eastern United States. The area has gently rolling topography from Kernersville to Greensboro, but becomes flatter towards Burlington. The climate of the area is humid subtropical. This climatic type is characterized by long, hot, humid summers, mild winters, and adequate and well-distributed precipitation throughout the year. The I-85/I-40 corridor between Kernersville and Burlington has an estimated population of about 1.1 million (NC magazine, 2010). There are 7 significant cities along the corridor: Kernersville, High Point, Thomasville, Randleman, Greensboro, Burlington, and Graham. Reidsville, Asheboro, and Siler City are within 40 miles of the I-85/I-40 corridor. This is evidence of the dramatic increase of urbanization in the region. The segment of the corridor is about

240 km (40 miles) long and about 300 km (50 miles) wide; it is one of the fastest growing regions in the state and ranks near the top nationally (NC magazine, 2010).

Figure 1. Road/Highway Map of the I-85/I-40 Corridor

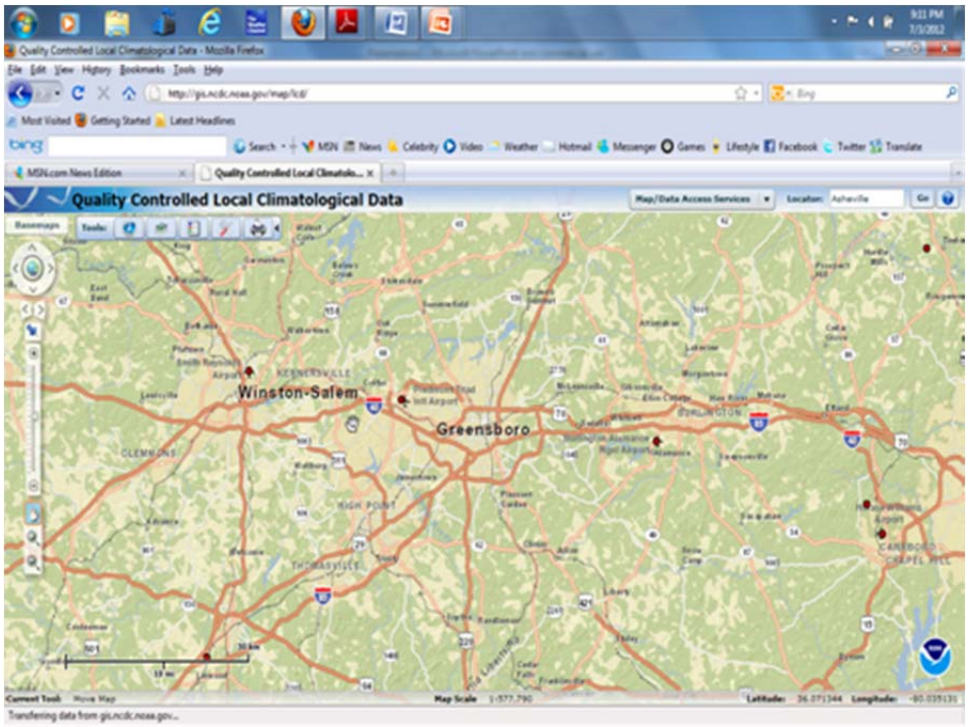

Source; National Climatic Data Center (NCDC); 2012

Figure 2. I-85/I-40 Corridor Study Area showing weather station locations

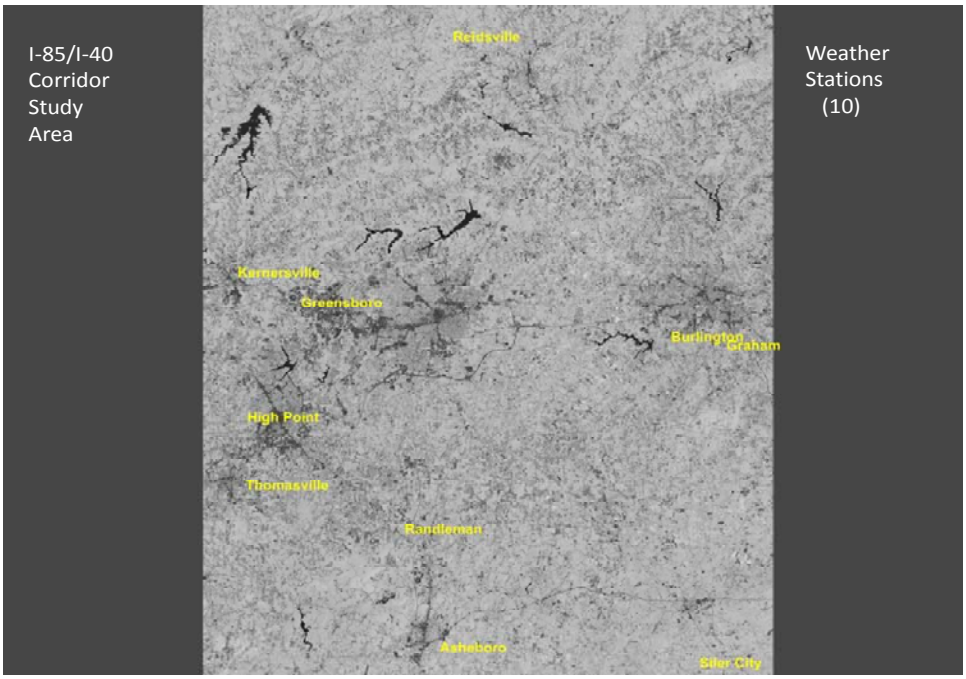

2.0. Data /Methodology---Acquiring/Processing Landsat Data

The I-85/I-40 corridor study used thermal data acquired from the NASA- Landsat (TM-5) sensors from the years 1990-1992 and 2000-2002. This structure parallels Streuker's (2003) study intervals of looking at and comparing data in 2 three-year segments. The images were acquired through the United States Geological Survey (USGS) Earth Resource Observation Data Center from the Earth Explorer and Global Land Cover Facility links.

Land surface temperature maps (LSTs) were created from the radiation data obtained from the selected satellite imagery (band 6-TM) and were used to determine the results and outcome of the urban heat island analysis of the I-85/I-40 corridor region. The TM sensors on board the Landsat satellites have three visible and four infrared sensors

with spatial resolutions of 30m and 120m thermal—band 6 (Aniello, 1994). The TM sensors on board the Landsat satellites scan in seven spectral bands (Table 1).

Table 1. Spectral Bands of the Landsat TM Sensor

Band	Spectral Range	Center of Range
1	Visible	.45µm
2	Visible	.52µm
3	Visible	.63µm
4	Near Infrared	.76µm
5	Mid-Infrared	1.55µm
6	Thermal Infrared	10.4µm
7	Mid-Infrared	2.08µm

The band 6 thermal (Landsat 4 &5) was used to determine land surface temperatures for this study. Thermal remote sensors observe the surface urban heat islands, or more specifically, they ‘see” the spatial patterns of upwelling thermal radiance received by the remote sensor (Voogt & Oke, 2003). Satellite-sensed temperatures are spatially averaged values, contrary to air temperatures, which are single point values measured in shelters at weather stations (Lee, 1992). Bands 3 and 4 were used to obtain the normalized difference vegetation indices (NDVI) from both rural and urban environments.

The vegetation index used in this study was the Normalized Difference Vegetation Index (NDVI); it was sampled over the urban and rural areas of the I-85/I-40 corridor for observing vegetation/impervious surface density and its relationship to UHI

development. The vegetation index was obtained from bands 3 (VIS) and 4 (NIR) of the Landsat Sensor using the following equation (Sobrino, 2004):

$$NDVI = (NIR - VIS)/(NIR + VIS)$$

where:
NDVI = Normalized Difference Vegetation Index
NIR = Band 4, Near-Infrared
VIS = Band 3, Visible

The NDVI equation produces values in the range from -1 to 1, where positive values indicate vegetated areas and negative values signify non-vegetated surfaces features such as water, urban, barren land, clouds and snow (Yuan & Bauer, 2007). NDVI is a surrogate for the amount of vegetation cover for photosynthetic potential (Xian & Crane, 2005).

The measurement of land surface temperature is affected by the differences in temperature between the ground and vegetation cover. Urban land surfaces possess diverse characteristics in both natural landscapes and man-made materials. These different surface elements have diverse energy budgets that generate apparent contrasts in surface characteristics and lead to complicated thermal patterns in urban areas. However, NDVI values would not be as useful during the winter months in environments where the vegetation is no longer green and photosynthetically active (Gallo et al, 1993).

NDVI seasonal measurements, thus, were calculated using selected images from the study's two time intervals and displayed on an Erdas Imagine map composition to show the temporal and spatial characteristics of the land cover/land use types relative to

the remotely sensed temperatures. Although the1 km spatial resolution of the AVHRR and the 30m and 120m spatial resolutions of the Landsat TM and ETM sensors are not detailed enough to resolve many surface features, the data are still useful for recognizing built up areas or parks, and surface temperatures can be located and applied to various climatic analyses (Lee, 1992). The UHI is detectable during morning hours, but is often more pronounced during afternoon and evening hours under clear, calm conditions (Oke, 1973). Because the descending pass of the satellite for the study region occurs between 0930--1000 EST (0430--0500 GMT), however, this study was limited to morning scenes (0 to 10% cloud cover).

Data collection and statistical analyses were conducted for this study by combining various methods from Lee (1992), Streuker (2003), Sobrino at al. (2004), Chen at al. (2005), Weng (2006) and Ahmad (2007), and Yuan and Bauer (2007). The study used two 3-year intervals (1990-1992 and 2000-2002), 10 years apart, in contrast to Streuker's (2003) study, which used two 3-year intervals that were 12 years apart. Streuker's study used 82 relatively cloud free images for his first interval and 125 relatively cloud free images for his second interval. Forty-six cloud-free images were available for the time intervals for this study; 11 images were from the 1990 interval and 12 were from the 2000 interval. Each of the 23 images contains bands 2, 3 and 4 plus 23 additional band 6 images (Table 2).

Once acquired, the raw images were unzipped and the bands were extracted. Bands 2 ,3,4, and 6 were extracted and the satellite imagery scenes are composed of bands 2,3, and 4 for the multiband images and band 6 for the thermal imagery. Each

scene was then subset to show only the study area and layer-stacked for multiband visualization. After these calibration procedures were completed, all the images were geometrically corrected, geo-referenced, and projected using the UTM projection system.

Table 2. Landsat Images available for the study

Date	Spring	Summer	Autumn	Winter
1990	April 13	August 3	October 6	December 19
1991	May 2	July 21	October 9	January 26
1992	May 4		October 27	March 2
2000	May 26	August 14	November 1	February 6
2001	March 26	September 18	October 20	February 6
2002	June 17	August 4	November 24	January 8

ERDAS IMAGINE was used to perform the geometric correction process; the results were resampled using bilinear interpolation.

3.0. Conversion Techniques--LST and NDVI

Radiance values from each of the Landsat thermal images were calculated by the following formula (Sobrino, 2004):

$$CVr = G\,(CV) + B$$

where:
CVr = radiance cell value
CV = cell value number
G = gain (0.005632156 for TM6 and 0.003705882 for ETM)
B = offset (0.1238 for TM6 and 0.32 for ETM)
Then, by applying Plank's equation of radiation (Sobrino,2004):

$$BT = K1/In\ (K2/CV2 + 1),$$

where:
BT = brightness temperatures in degrees Kelvin
CVr = radiance value
K1 = calibration coefficient (60.776 for TM and 666.09 for ETM)
K2 = second calibration coefficient (1260.56 for TM and 1282.71 for ETM)

the radiance values were converted to brightness temperature (radiometric temperature) values.

Atmospheric factors and surface emissivity can influence the land surface temperature estimation and would probably cause incorrect measurements in the calculations proposed (Stathopoulou & Cartalis, 2004). Knowledge of the land cover/land use type is very important for the determination of surface emissivity, which has a direct relationship with surface temperatures (Stathopoulou & Cartalis, 2004). Surface emissivity is known to be an important factor in radiance balance and transfer (Yang & Wang, 2000).

Emissivity is basically the emitting ability of an object or surface, compared to that of a blackbody at the same temperature. The effect of land surface emissivity on satellite measurements can be generalized into three categories: (1) emissivity causes a reduction of surface emitted radiance; (2) non-black surfaces reflect radiance, and (3) the anisotropy of reflectivity and emissivity may reduce or increase the total radiance from the surface (Prata, 1993 & Weng, 2009). Water content, chemical composition, and structure are some factors that controls the emissivity of a surface. Emissivity can vary significantly with plant species, areal density, and growth stage (Snyder et al., 1998 &

Weng, 2009). On the other hand, emissivity is a function of wavelength, commonly known as spectral emissivity.

Emissivity for ground objects from passive sensor data has been estimated using different techniques such as the (1) NDVI method; (2) classification-based estimation, and the (3) temperature-emissivity separation model. These techniques are applicable to separate temperature from emissivity, so that the effect of emissivity on estimated LST's can be determined (Weng, 2009). The Earth's surface is comprised of complicated land-use and land cover types, and the surface emissivities are difficult to measure accurately (Yang, 2007). It seems more appropriate to correct the effect of spectral emissivity on LST's derived from thermal remote sensing imagery by assigning an emissivity value to each land cover category (Snyder et al, 1998). According to Oke (1987), emissivity values for vegetation ranges from .97 to .99, whereas values for urban materials (concrete, asphalt, and stone) range from .95 to .96. Emissivity values of every land category ranges from 0.95 to 0.99 according to most previous UHI studies (Nichol, 1996; Zhang, 2006). However, Streuker (2003) mentioned in his study that a difference in emissivity of at least 0.01 to 1 is quite likely and would thus cause the UHI magnitudes to be underestimated by a degree or two.

Table 3. Emissivity values for selected land covers/land uses

Class	Value	
Water	.99	
Heavy Urban	.96	
Light Urban	.97	
Barelands/Fields	.98	
Forest/Vegetation	.99	

This study also obtained and utilized emissivity values to get more accurate LST's. Sobrino's NDVI Threshold Methods was used to calculate the emissivity values from the NDVI considering different cases. Both Planck's equation of radiation and Sobrino's equation have been extensively used with much success in several urban heat island studies (Streuker, 2003; Gallo, 1997; Lee, 1992; Stathopoulou & Cartalis, 2007; and Ahmad, 2007

The case that was used in this study was when the pixel was composed by a mixture of bare soil and vegetation. The emissivity was calculated according to the following equation (Sobrino, 2004):

$$e=EvPv + Es\ (1-Pv) + de$$

where:
Ev = vegetation emissivity
Es = soil emissivity
Pv = vegetation proportion obtained from the NDVI equation (NDVI - NDVImin /NDVImax - NDVImin), where NDVImax = 0.5 and NDVImin = 0.2,
de = geometrical distribution of the natural surfaces (homogeneous vs. heterogeneous).

The results from the emissivity equation that were used in this study were: (1) Esoil (soil emissivity) = .97 when NDVI < 0.2; (2) Eveg (vegetation emissivity) = .99 when NDVI >0.5and .98 when NDVI values were between 0.2 and 0.5, (Ahmad, 2007). NDVI values between -1 and .1 have emissivity values around .95 and .96, which represents the urban/built-up areas (Zhang et al, 2006). The assigned emissivity values for land

cover/land use surfaces for this study were: water--0.99; forest--0.98; barelands/fields--0.97; light urban--0.96; and heavy urban--0.95. The emissivity values assigned to the LST equation for this study were 0.98 for the spring/summer/fall seasons and .97 for the winter seasons. Initial LST values were computed using Kelvin (K) degrees, then were modified by subtracting 273.15 to derive LST centigrade (C) values, which were used in the creation of the LST maps. The final products from these processes were distinct temperature datasets of remotely sensed land surface temperatures from each of the 23 images, including the cities and surrounding areas of the corridor study region. The brightness temperatures from TM band 6 thermal were then used to calculate the land surface temperature using the Sobrino equation (Ahmad, 2007):

$$Ts = BT/(1+ (W \times BT/p)\ln e$$

where:
Ts = land surface temperature
BT = at-sensor brightness temperature (K)
W = wavelength of emitted radiance (11.5um);
ln *e* = Log of the spectral emissivity value

4.0. Unsupervised LCLU Classifications

Land cover/Land use classifications (LCLU) were performed for each scene used in this study. Unsupervised classifications were computer- generated, with the software identifying statistical patterns in the data without using any ground truth data. One of the options that ERDAS IMAGINE uses to create the classifications is the Isodata algorithm. The Isodata clustering method uses the minimum spectral distance formula to form

clusters. It begins with either arbitrary cluster means or the means of an existing signature set. As the clustering repeats each time, the means of these clusters are shifted. The new cluster means are then used for the next iteration (Jensen, 2004). The Isodata algorithm repeats the clustering of the image until a maximum percentage of unchanged pixel assignments has been reached between two iterations. Ten iterations were used because of the time factor involved in running the clustering method. Bands 3 and 4, not the whole data set, are used in the classification scheme because the land cover information is located in these bands which are visible and near infrared respectively. Accuracy of the land classifications were based on historical data (Google Earth, 2012) of the corridor study area and accuracy assessment tasks that were performed in Erdas Imagine. The tasks are the overall classification accuracy, error matrix, and kappa statistics. The classification overlay procedure was also utilized in which the classified image is overlayed with the original image for land cover/land use comparison.

5.0. Weather Station Archived Data

Weather station-archived hourly minimum temperature datasets are the second set of temperature data that was used and analyzed in this study. The weather station data were downloaded from the Southeast Region Climate Center (SERCC) and the State Climate Office of North Carolina (SCONC) websites. The archived hourly minimum temperature data was acquired from the ten (10) weather stations in the corridor area (Table 4; Figure 1). The weather station data was used for ground truthing and examining their relationships to the satellite-derived LST data

The archived hourly weather data was only available for the 2000 interval (2000-2002), so comparisons for this aspect of the study worked with a subset of the original imagery. A UHI intensity analysis (Table 5) was performed using the archived hourly temperatures of three selected urban/rural locations for the 2000-2002 interval as an initial step to see if any UHI activity was present in the region. These three urban/rural sites represents the three largest cities in the corridor study area (Greensboro, High Point, and Burlington) along with the nearest rural site for each large city. Those rural sites are Kernersville, Thomasville, and Graham respectively. The winter seasons of the 2000 interval have LST's and hourly minimum temperatures that are within 4 degrees of each other. The spring, summer and autumn seasons of the 2000 interval have LST's and hourly minimum temperatures that are within 9 degrees of each other (Tables 6-8). Oke (1991) argues that the intensity of an UHI can be quantified by the maximum difference between urban minimum temperature and the rural minimum temperature. Of the three locations, Greensboro/Kernersville recorded the highest UHII (1.433), Burlington/Graham (.833), and High Point/Thomasville (0.179). The distance between the urban and rural weather stations was no more than 7 miles. Even though the UHI intensity is small between these urban and rural locations, it appears to be increasing.

Table 4. Latitude, Longitude, and Altitude of the 10 weather stations located in the I-85/I-40 Corridor

Weather Station	Latitude	Longitue	Altitude	WX Location
Asheboro	35.42	-79.47	673	Randolph Cty Airport
Burlington	36.05	-79.25	617	Alamance Cty Airport
Graham	36.02	-79.23	660	Swepsonville Fork N of 87
Greensboro	36.05	-79.57	926	PTI Airport
High Point	35.59	-80.02	980	Shadow Valley/Lindale Farms
Kernersville	36.08	-80.02	935	Smith Reynolds Airport/Harvest Ridge
Randleman	35.49	-79.49	810	Pleasant Garden
Reidsville	36.24	-79.45	858	Reidsville EMS
Siler City	35.39	-79.25	614	Siler City Airport
Thomasville	35.53	-80.01	733	Davidson Cty Airport

Table 5. Corridor Cities—Urban vs. Rural (Hourly Minimum Temperatures—1000am (UHII—Urban Heat Island Intensity)

	Greensboro vs. Kernersville	Burlington vs. Graham	High Point vs. Thomasville
2/2/00	38/41	34/34	40/40
5/26/00	73.9/73	74/74	74/73
8/14/00	77/74.3	76/75	76.3/75.5
11/2/00	57/57.4	57.7/56.3	56/55.7
2/6/01	42.1/37	41/40	42/42
3/26/01	38/37	41/40	38/38
9/18/01	74/73	75/73	72/72
10/20/01	60.1/59	63/61	59/59
1/8/02	30/30	32/32	32/32
6/17/02	75/76	78.1/78	76/75.7
8/4/02	83/83	83/83	83/83
11/24/02	52/42	51.1/49	51/51
	UHII +1.433	UHII +0.883	UHII +.079

Table 6. Hourly Minimum Temperatures versus Satellite Land Surface Temperatures
Year 2000 MinTemps/ LST's (930-1000am)-(degrees C)

	Feb. 6, 2000	May 26, 2000	Aug 14, 2000	Nov. 1, 2000
Asheboro	4/6	23/25	25/26	15/17
Burlington	1/5	23/29	24/26	14/16
Graham	1/6	24/28	24/24	13/15
Greensboro	3/5	23/25	25/29	14/18
High Point	4/4	23/24	25/24	13/16
Kernersville	5/6	23/25	24/24	14/17
Randleman	4/6	22/26	24/28	12/17
Reidsville	4/5	22/27	24/22	14/14
Siler City	4/5	22/24	24/26	14/15
Thomasville	4/6	23/25	24/23	13/15

Table 7. Hourly Minimum Temperatures versus Satellite Land Surface Temperatures Year 2001
MinTemps/ LST's (930-1000am)-(degrees C)

	Feb. 6,2001	Mar. 26,2001	Sept. 18,2001	Oct. 20, 2001
Asheboro	6/7	6/12	23/21	21/21
Burlington	5/5	5/12	24/24	17/25
Graham	4/4	4/9	23/23	16/22
Greensboro	6/6	3/9	23/27	16/26
High Point	6/7	3/10	22/27	15/25
Kernersville	6/5	3/8	23/23	15/23
Randleman	5/8	5/10	23/24	20/22
Reidsville	6/6	2/8	23/21	15/22
Siler City	6/6	5/12	24/21	20/21
Thomasville	6/5	3/10	22/24	15/23

Table 8. Hourly Minimum Temperatures versus Satellite Land Surface Temperatures Year 2002 MinTemps/ LST's (930-1000am)--(degrees C)

	Jan. 8,2002	June 17,2002	Aug. 2,2002	Nov.24,2002
Asheboro	1/1	26/clouds	29/25	10/13
Burlington	0/-1	26/28	28/27	11/11
Graham	0/-3	26/27	24/26	9/11
Greensboro	1/-1	24/27	28/29	9/12
High Point	0/0	24/24	28/27	11/12
Kernersville	1/-4	24/22	23/27	6/10
Randleman	0/-1	25/27	28/23	9/10
Reidsville	-1/-2	24/24	28/27	6/10
Siler City	1/-4	27/19	28/23	10/12
Thomasville	0/-4	24/23	28/24	11/11

In addition to the UHI intensity analysis, several locations were sampled for LST values on the imagery (Table 9) in an effort to provide a more comprehensive picture of temperature variations. These locations included including airport areas, lakes, rural locations, and highways.

Figure 3. The 15 Selected Locations of the I-85/I-40 Corridor Study Area

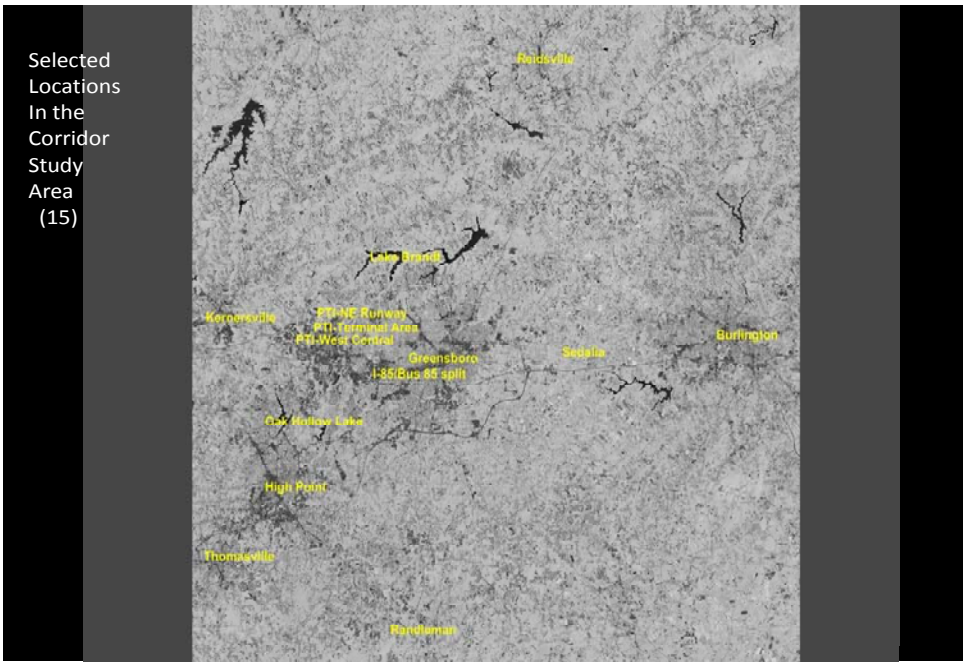

Table 9. Latitude and Longitude of Selected Locations in the I-85/I-40 Corridor Study Area

Selected Locations	Latitude	Longitude
PTI –W Central	36 05.54	79 56.51
PTI-Terminal Area	36 05.50	79 56.16
PTI-NE Runway	36 06.47	79 55.05
Business 85/I-85 split	36 03.24	79 49.47
Downtown Asheboro	35 41.34	79 48.59
Downtown Burlington	36 05.13	79 25.45
Downtown High Point	35 57.15	80 00.17
Lake Brandt (G'boro)	36 10.25	79 51.30
Oak Hollow Lake (HP)	36 01.06	79 59.39
Downtown Kernersville	36 07.13	80 04.18
Sedalia	36 04.42	79 37.37
Downtown Reidsville	36 21.13	79 39.53
Downtown Greensboro	36 04.17	79 47.26
Randleman	35 48.55	79 48.35
Thomasville	35 53.03	80 04.34

Table 10. Selected Locations (15) and Land Surface Temperatures (Celsius) in Corridor Study Area (1991 vs. 2001--Autumn--1000am DST)

Selected Locations	**Image 1991282** (October 9, 1991)	**Image 2001293** (October 20, 2001)
PTI –W Central	19.670	27.323
PTI-Terminal Area	20.559	26.882
PTI-NE Runway	17.420	24.205
Business 85/I-85 split	21.001	25.995
Downtown Asheboro	20.559	25.103
Downtown Burlington	19.670	25.995
Downtown High Point	21.441	29.073
Lake Brandt (Gboro)	12.797	18.681
Oak Hollow Lake (HP)	15.130	18.681
Downtown Kernersville	21.001	26.882
Sedalia	14.202	20.008
Downtown Reidsville	19.223	25.550
Downtown Greensboro	21.001	26.882
Randleman	16.509	23.300
Thomasville	22.319	29.073

6.0. Statistical Analysis

Preliminary assessments of the changes in LSTs for a selected set of locations across the imagery suggest the probability of UHIs in the region. To examine this in further detail, possible relationships between LSTs and NDVIs were investigated. A subset of the available imagery was selected for both the descriptive comparisons as well as the final statistical analysis. For the descriptive comparisons, this study focused on imagery from 1990 and 2000 as these pairs were largely representative of changes for all pairs. For the statistical analysis, the imagery subset was further narrowed to examine four seasons of one specific year to investigate relationships across those seasons. Following the methods of Yuan and Bauer (2007), a set of 5000 points were randomly sampled for the region. These points were used to extract LST and NDVI

values from the displays created from the satellite imagery. Once extracted, the NDVI points were plotted against the LSTs to examine how well these values might correlate to LSTs. Then, to further investigate the relationship between LSTs and NDVI values, a zonal analysis was conducted to assess the mean LST values against small NDVI increments (0.01, from -1 to 1).

Table 11. Selected Locations (15) for Land Surface Temperatures (Celcius) in Corridor Study Area (1992 vs. 2002--Spring-1000am DST)

Selected Locations	**Image 1992125** (May 4, 1992)	**Image 2002168** (June 17, 2002)
PTI –W Central	19.421	31.203
PTI-Terminal Area	20.228	29.138
PTI-NE Runway	17.670	27.043
Business 85/I-85 split	21.578	30.793
Downtown Asheboro	20.719	cloud cover
Downtown Burlington	22.005	28.304
Downtown High Point	21.578	34.046
Lake Brandt (Gboro)	12.267	20.115
Oak Hollow Lake (HP)	12.267	20.115
Downtown Kernersville	22.005	33.239
Sedalia	12.267	22.319
Downtown Reidsville	20.228	31.613
Downtown Greensboro	23.700	32.834
Randleman	13.640	cloud cover
Thomasville	24.121	33.643

Table 12. Selected Locations (15) for Land Surface Temperatures (Celcius) in Corridor Study Area (1990 vs. 2000--Summer--1000am DST)

Selected Locations	**Image 1990215** (August 3, 1990)	**Image 2000227** (August 14, 2000)
PTI –W Central	27.885	31.657
PTI-Terminal Area	27.043	29.939
PTI-NE Runway	24.916	27.762
Business 85/I-85 split	18.325	32.508
Downtown Asheboro	23.623	25.103
Downtown Burlington	28.722	29.939
Downtown High Point	27.043	31.229
Lake Brandt (Gboro)	18.775	23.753
Oak Hollow Lake (HP)	20.115	23.753
Downtown Kernersville	25.344	30.371
Sedalia	27.885	29.507
Downtown Reidsville	27.043	30.801
Downtown Greensboro	28.772	31.229
Randleman	23.190	21.932
Thomasville	27.043	30.801

Table 13. Selected Locations (15) for Land Surface Temperatures (Celcius) in Corridor Study Area (1991 vs. 2001--Winter--1000am EST)

Selected Locations	**Image 1991026** (January 26, 1991)	**Image 2001037** (February 6, 2001)
PTI –W Central	-0.865	6.615
PTI-Terminal Area	-0.350	6.132
PTI-NE Runway	-1.382	5.646
Business 85/I-85 split	-0.865	5.159
Downtown Asheboro	0.162	6.615
Downtown Burlington	-1.902	6.615
Downtown High Point	-0.350	5.646
Lake Brandt (Gboro)	-0.350	1.180
Oak Hollow Lake (HP)	0.162	0.672
Downtown Kernersville	-0.350	7.097
Sedalia	-1.902	4.669
Downtown Reidsville	0.162	0.672
Downtown Greensboro	-0.350	6.132
Randleman	-2.424	4.117
Thomasville	1.180	9.003

CHAPTER IV

RESULTS AND DISCUSSION

1.0. Land Surface Temperatures

This study investigated the presence of urban heat island climates in the I-85/I-40 corridor area and their growth and /or change between 1990 and 2000 by observing the spectral and thermal signatures of rural and urban land cover types. One of the first steps in this investigation was preparing sets of maps to visualize variation in LST values over time across the region. These maps paint pictures of the spatial extent of the UHI effect for the region, as well as offer insight into the range of surface temperatures. What follows is a summary of findings for those image pairs most closely matched in dates of acquisition.

In the 1991 autumn image (Figure 4), for example, the highest temperatures were located in the downtown areas of High Point (21.4), Thomasville (22.3), Greensboro (21.0), and Kernersville (21.0). The autumn image from 2001 (Figure 5) suggests substantial increases in LSTs for these downtown hot spots, with High Point recorded as 29.0, Thomasville as 29.0, Greensboro as 26.9, and Kernersville as 26.9. In addition to the downtown areas, several other locations were sampled, including airport areas, lakes, rural locations, and highways (Table 9) in an effort to provide a more comprehensive picture of temperature variations. In each of these locations, LSTs were warmer in the 2001 image than the 1991 image (Table 10).

Figure 4. 1991282 October 9, 1991--Autumn--945am DST

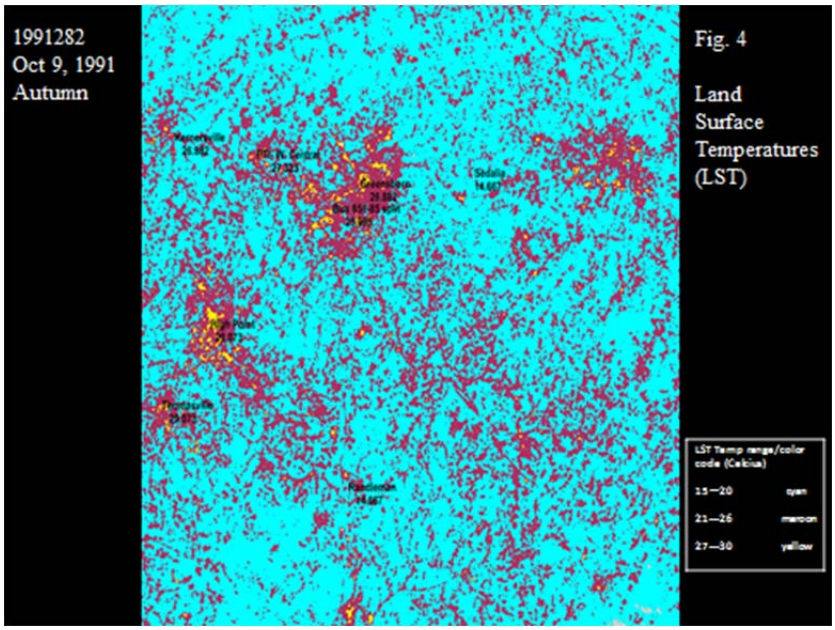

Figure 5. 2001293 October 20, 2001--Autumn--945am DST

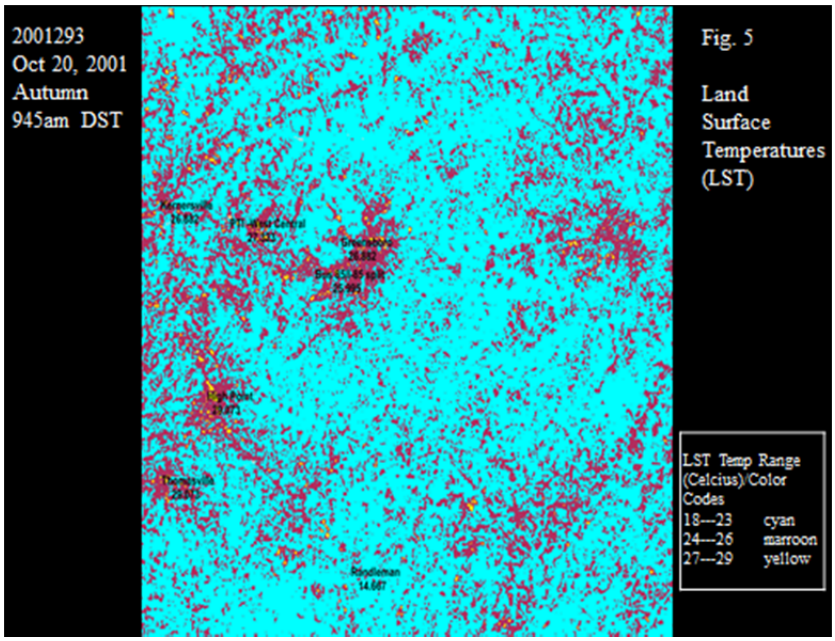

A comparison of the best summer season images (Figures 6 and 7) suggested patterns similar to those from the autumn comparisons. The 2000 image generally had warmer LST values than the 1990 image. The warmest temperatures occurred at the Bus 85/I-85 split (32.508). One factor to support this is usually around 930-1000am at this location every morning, there is a large volume of traffic on both highways going both directions. Other warm temperatures occurred in downtowns Greensboro and High Point (31.2), Reidsville and Thomasville (30.8), Kernersville (30.4), Burlington (29.9) and along with the west central PTI airport area (31.7). Lakes Brandt and Oak Hollow had among the coolest LST values (23.8 for both), again mirroring the results from the autumn images. The 1990 image has cooler temperatures than the 2000 image. Greensboro (28.772), High Point (27.043), and Thomasville (27.043) were the warm urban areas in the 1990 image along with PTI--West Central area (27.885) and the Bus 85/I-85 split (27.465). Lakes Brandt (12.267) and Oak Hollow (23.544) have the cooler temperatures along with Sedalia (24.699) and Randleman (25.348).

For the spring season, the 2000 image LST's were at least twice as high (much warmer) as the 1990 image LST values at all locations (Figures 8 and 9). Downtown Kernersville recorded the warmest LST value (36.944), followed by Downtown Greensboro and Reidsville (35.701 for both) and both downtowns of High Point and Thomasville (36.531). The I-85/Business 85 split again has the warmest LST value (36.944) during this period. The PTI airport was fairly warm as well in all three areas--west central (34.027), terminal area (33.183), and northeast runway (31.051).

Figure 6. 1990215 August 3, 1990--Summer--945am DST

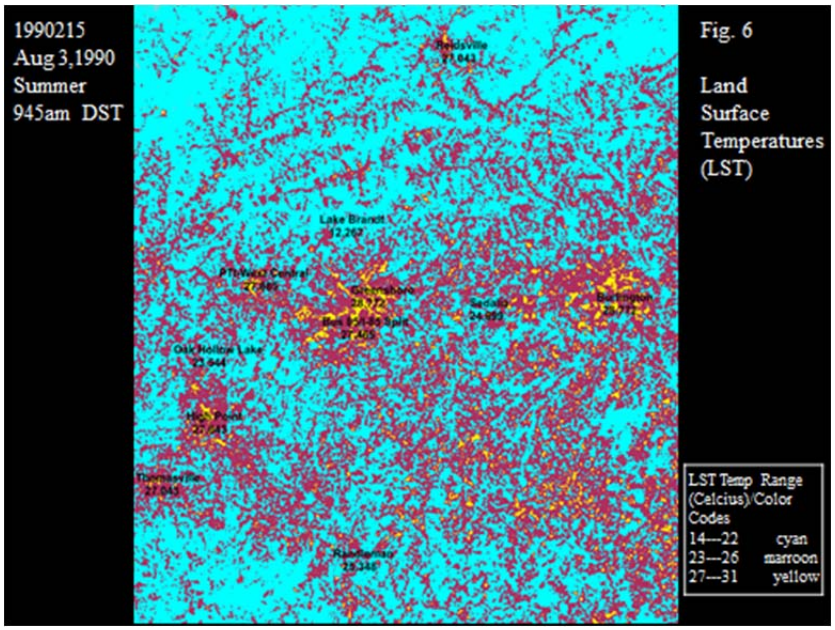

Figure 7. 2000227 August 14, 2000--Summer--945am DST

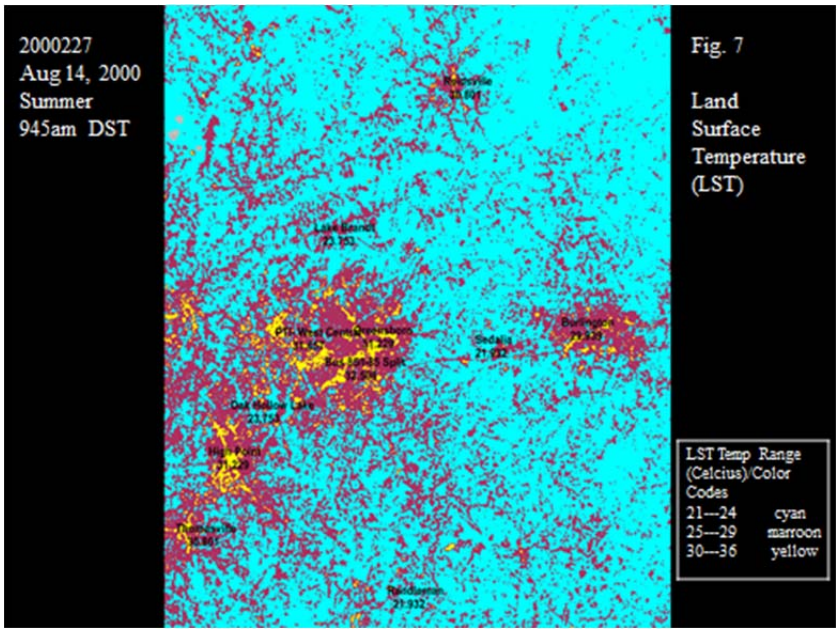

Figure 8. 1990103 April 13, 1990--Spring--945am DST

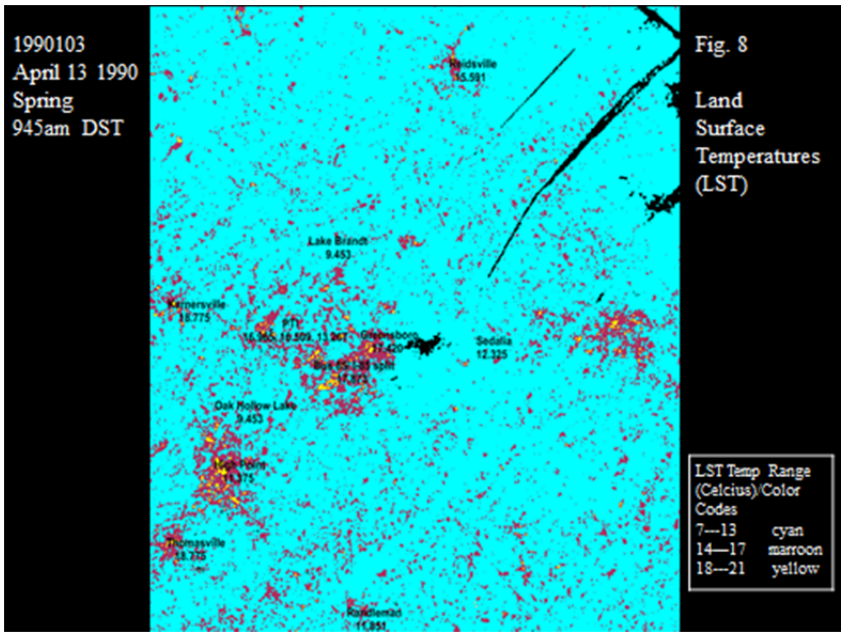

Figure 9. 2000147 May 26, 2000--Spring--945am DST

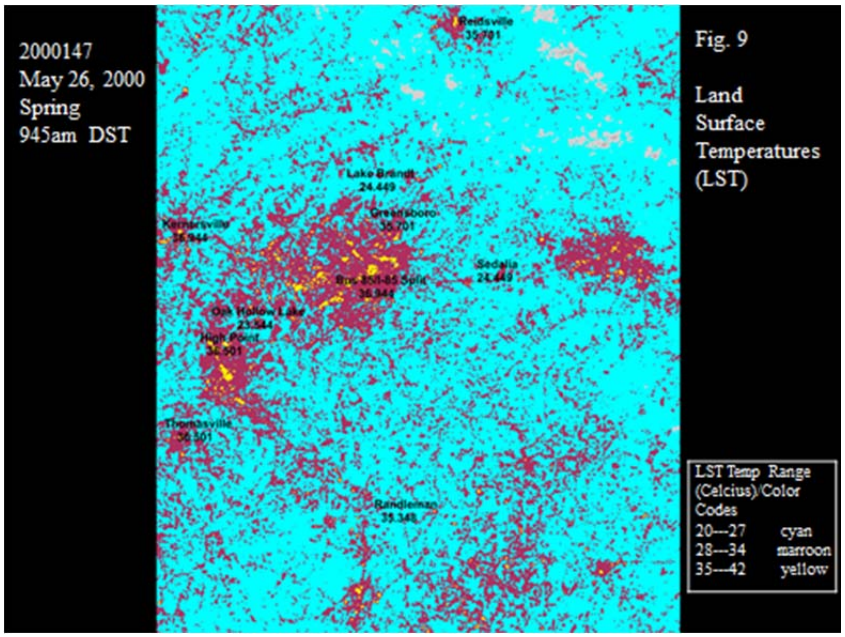

Oak Hollow Lake and Lake Brandt continue to have the lowest LST values of 23.544 and 24.449 respectively. The rural locations of Sedalia and Randleman follow with low LST values of 24.899 and 25.348. LSTs from the 1990 image include Kernersville (18.775), Thomasville (18.775), and Asheboro (18.325) which have the warmest temperatures among the urban centers. Bus 85/I-85 split (17.873) and the PTI–West central and terminal areas (16.965 & 16.509 respectively) also have warm temperatures. Lakes Brandt and Oak Hollow (9.453 for both) again have the cooler temperatures along with Randleman (11.851) and Sedalia (12.325). One interesting point is that, climatologically, 1990 and 2000 were among the hottest years during the past 25 years in the corridor area with 2000 being the hottest of the two. Similar results were obtained with the 1992 and 2002 spring images.

Finally, for the winter season, the 2001 image has warmer temperatures than the 1991 image (Figures 9 and 10). The winter LST values varied significantly all over the corridor study area. Warmer LST values in the 2001 image were at the PTI locations (5-7), I-85/I- 85 Business split (5.159), and the urban corridor centers of Thomasville (9.003) and Kernersville (7.097). Lake Brandt and Oak Hollow Lake had the lowest LST values of 1.180 and 0.672 respectively. The rural location of Sedalia also had a low LST value of 4.669. The warmer areas of the 1991 image occurred in Thomasville (1.180) and Reidsville (0.672). Lakes Brandt and Oak Hollow (0.350 & -0.162 respectively) along with Sedalia (-1.902) and Randleman (-2.424) had the coldest temperatures for the 1991 image.

Figure 10. 2001037 February 6, 2001--Winter--945am EST

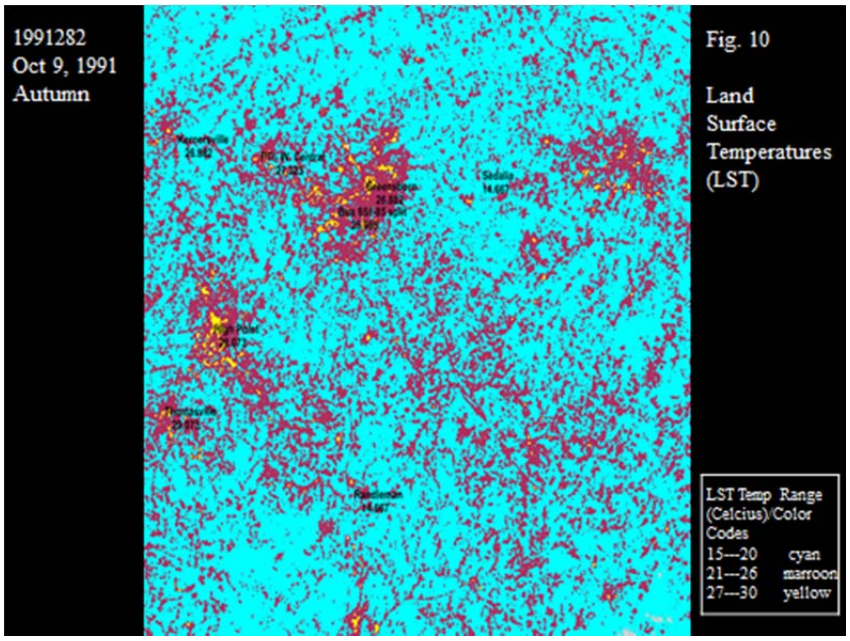

Figure 11. 1991026 January 26, 1991--Winter--945am EST

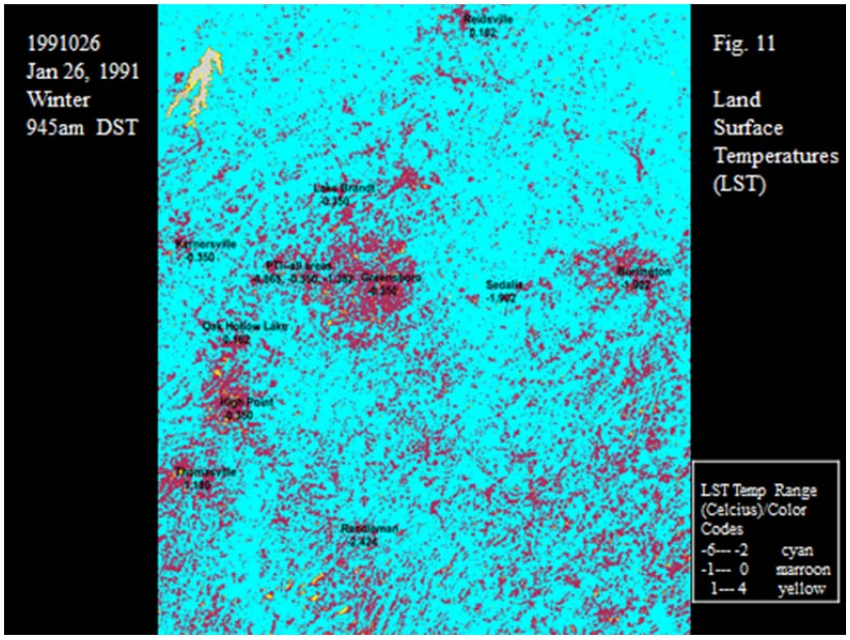

Overall, the winter LST values for the 2001 image were dramatically higher than the 1991 values, however, the LST values for Lakes Brandt and Oak Hollow along with the rural locations of Sedalia and Randleman always were the coolest areas.

Air temperature data from the ten weather stations were also compared to the LST temperatures. LST values for the weather station locations were a few degrees higher than the archived hourly minimum air temperatures in all the 2000 images. This is reasonable since daytime land surface temperatures are generally warmer than the air temperatures (Yuan & Bauer, 2007). However, regressing the original LST values to derive adjusted LST values would probably get the LST values even closer to the in situ minimum temperature values but this procedure was not performed in this study. The 1990 and 2000 summer and spring images generally had higher LST values than the 1990 and 2000 autumn and winter images. The summer, spring and autumn images indicated various “hot spot” areas throughout the study area with most occurring in the corridor urban centers and along the I-40/I-85 interstate corridor. These “hot spots” suggest thermals that are derived from surface heat fluxes and anthropogenic heat sources that could be possible urban heat island climates. There are several reasons to support this claim--(1) The” hot spot” areas are warmer than the surrounding areas by several degrees; (2) sensible heat storage has increased because of higher thermal admittance to building and construction materials; (3) anticyclonic conditions (high pressure) is present in all the images and the resultant strong solar radiation helps to increase the growth of these thermal climates; and (4) total turbulent heat fluxes have decreased due to lack of wind speed in these selected images.

2.0. Unsupervised Classifications

Maps were also prepared to visualize land cover and land use for the region and to compare the various categories to LST variation across the region. Using unsupervised classification, five classes were chosen for the identification and display of the spectral signatures of land cover/land use types--heavy urban, light urban, forest/vegetation, barelands/fields, and water. Of the images classified for comparative study, the majority of image pairs highlighted similar findings. Thus, image pairs from 1990 and 2000 were chosen to highlight those findings here.

Comparing the autumn images from 1990 and 2000 (Figures 12 and 13), substantial light urban buildup, expanding from 3% to 13% can be seen in Greensboro, High Point, and Burlington in the 2000 image (Table 13). Kernersville has significant buildup of light urban (residential) use in 2000 as well, especially more residential development. Other areas where urban buildup is noticeable in 2000 include Piedmont Triad International Airport (PTI), including residential buildup on the southern and southeastern periphery areas near the airport, Greensboro's CBD to east and west Greensboro, and High Point's urbanization from downtown to the north/ northeast and south. Burlington shows more residential and commercial growth north of the city.

Table 14. Unsupervised Classification Percentages, Autumnal Seasons

Autumn		
	Oct. 1990	Nov. 2000
Water	1%	1%
Heavy Urban	10%	9%
Light Urban	3%	13%
Barelands/Fields	11%	7%
Forest/Vegetation	75%	70%

Reidsville has less barelands/fields land cover in 2000 than in 1990, which matches the overall trend in the images, with barelands and fields shrinking from 11% to 7%.

Figure 12. LCLU Classification, Autumn Image 1990279--October 6, 1990

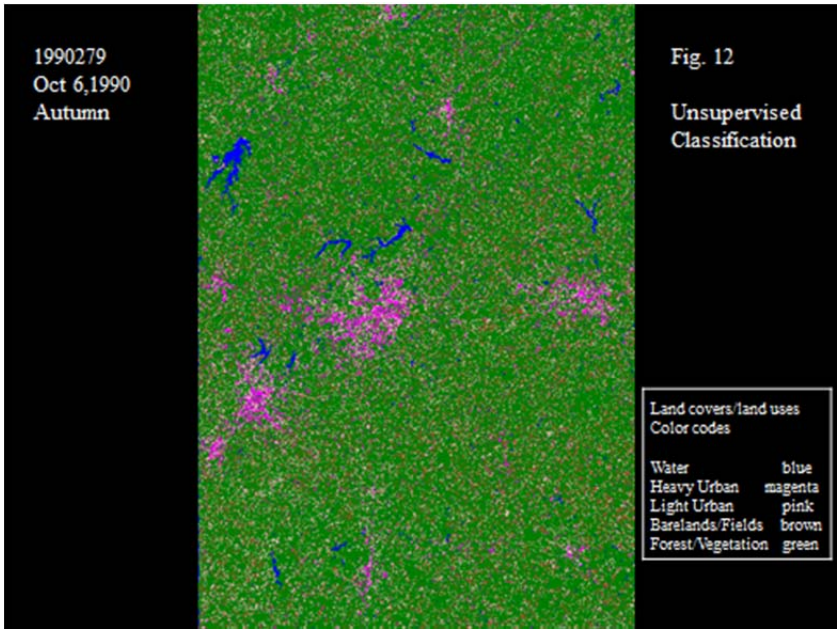

Figure 13. LCLU Classification, Autumn Image 2000307--November 1, 2000

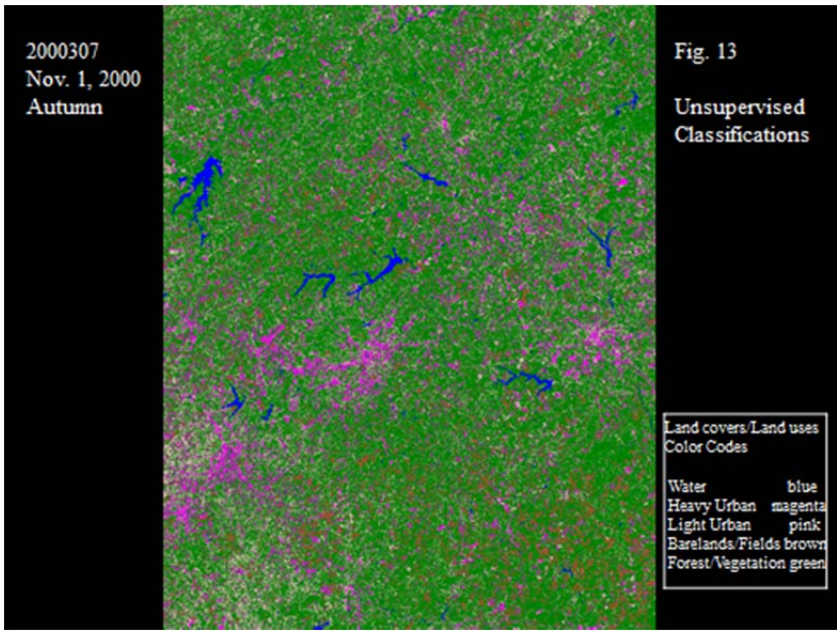

Accuracy Assessment tasks were performed on the October 1990 and November 2000 Unsupervised images. These tasks consisted of an overall classification accuracy, Kappa statistics, and error matrix reports. The classification accuracy report calculates the statistics of the percentages of accuracy relative to the error matrix results. The error matrix report simply compares the historical (reference) values to the assigned class values. Kappa statistics measured the ability to provide information about a single matrix as well as to statistically compare matrices (Congalton, 1991). Historical reference images were utilized to evaluate the classification accuracy of the selected images. The historical images were obtained from the Google Earth link. The March 1993 historical image was selected to confirm the October 1990 classification. The March 2000 historical image was selected to confirm the November 2000 classification. Results from the assessment revealed that the overall classification accuracy of the October 1990

image is 82% and the Kappa statistics are 0.7374 (74%). The overall classification accuracy of the November 2000 image is 87% and the Kappa statistics are 0.8178 (82%). The error matrix reports (Table 14) indicates the accuracy of the classes between the reference and classified images. These accuracy results confirmed the land cover/ land use changes that occurred from 1990 to 2002 in the corridor study area. It also confirmed that the classification percentages are accurate as well. Finally, the results also indicate the high accuracy percentages of the spring and summer classification images used in this analysis since they all were created by the same tasks, methods and procedures.

Table 15. Accuracy Assessment Error Matrix Reports

March 93/October 90 -- Error Matrix Report			
Class	Ref totals	Class totals	No. of corr
Water	10	10	10
Heavy Urban	52	48	43
Light Urban	14	15	10
Barelands/Fields	7	12	5
Forest/Vegetation	17	15	14
March 00/November 00—Error Matrix Report			
Class	Ref totals	Class totals	No. of corr
Water	8	10	8
Heavy Urban	46	46	41
Light Urban	14	16	13
Barelands/Fields	15	15	14
Forest/Vegetation	17	13	11

Like the autumn image comparison, the two summer images (Figures 14 and 15) suggest an increase in light urban buildup, from 6% to 11% (Table 15). In these images, commercial and residential development west of Greensboro and east of PTI airport, north and northwest of High Point, and periphery areas all around Burlington appears

more spread out and heavier on the 2000 map. However, the Asheboro and Randleman areas show very little change during this period. Both barelands/fields land cover and forest vegetation cover appear to decrease slightly from 1990 to 2000.

Table 16. Unsupervised Classification Percentages, Summer Seasons

Summer			
	Aug. 1990	Aug. 2000	Aug. 2002
Water	1%	2%	2%
Heavy Urban	2%	5%	7%
Light Urban	6%	11%	11%
Barelands/Fields	19%	3%	10%
Forest/Vegetation	72%	79%	70%

The 2002 summer image (Figure 16) was also compared to the 1990 summer image. Light urban buildup (residential development) increased from 6% in 1990 to 11% in 2002 and is noticeable in Greensboro, High Point, Burlington, and Kernersville, although little change is apparent for Reidsville and Asheboro. Heavy urban buildup (commercial development/road construction/ airport development) increased from 2% in 1990 to 7% in 2002. Thomasville shows some minor residential development in various sectors of the city. Forest/vegetation appears to increase slightly as well in the 2002 image, while barelands/fields land covers decreased.

Figure 14. LCLU Classification, Summer Image 1990215--August 3, 1990

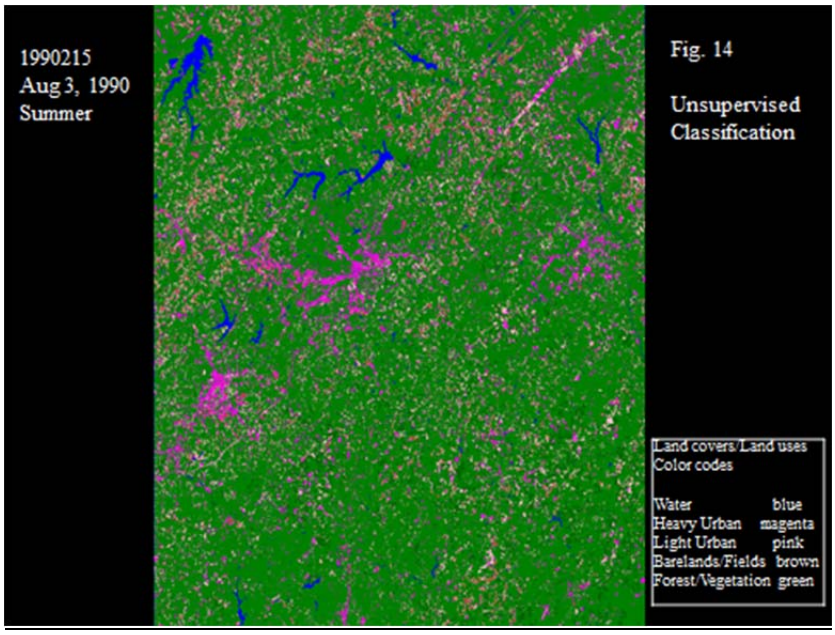

Figure 15. LCLU Classification, Summer Image 2000227--August 14, 2000

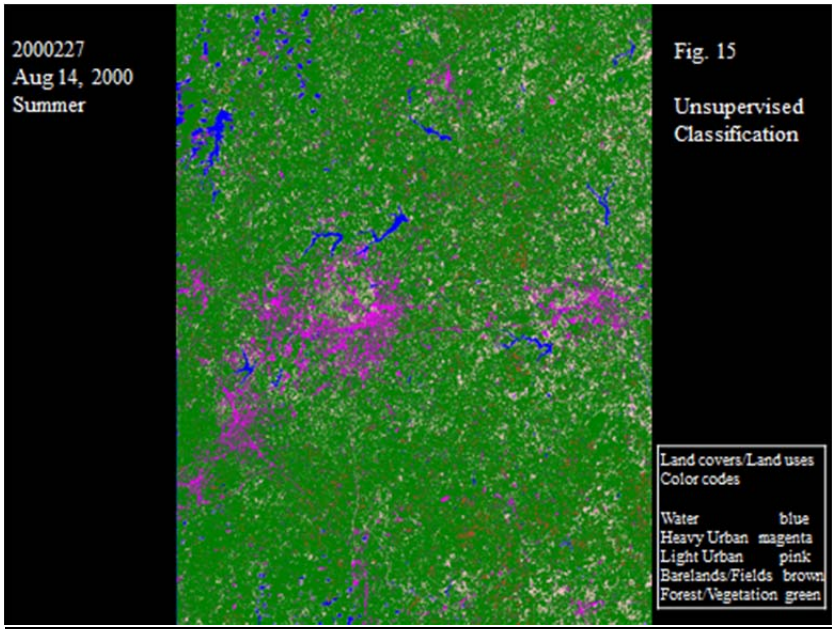

Figure 16. LCLU Classification, Summer Image 2002216--August 4, 2002

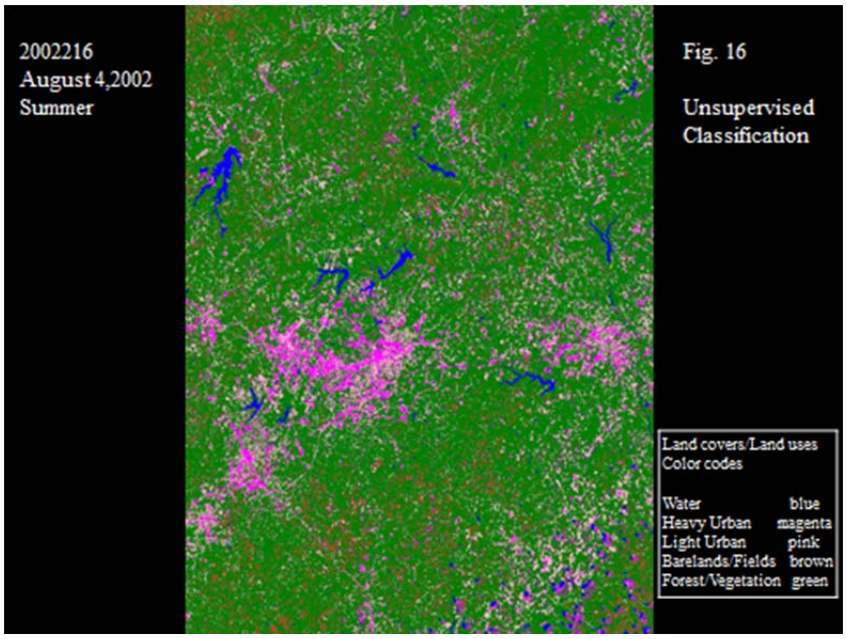

The 2000 spring image (Figure 18), compared to the 1990 image (Figure 16), shows a 4% increase in light urban buildup (Table 15). Moderate light urban land use is evident south of the Triad in the 2000 image, with forest/vegetation land cover more prevalent in the 1990 image. Heavy urban development is more pronounced visually than light urban development in the 1990 image. Kernersville and Thomasville show more light urban development in 2000 than 1990.

Finally, the 2000 winter image (Figure 20) showed increased light urban land use relative to the 1990 image (Table 16), which is evident in all the corridor urban centers. Barelands/fields land cover shows little change between the two images. Forest/vegetation land cover also shows little change between the two images.

Table 17. Unsupervised Classification Percentages, Spring Seasons

Spring		
	Apr. 1990	May 2000
Water	1%	1%
Heavy Urban	7%	3%
Light Urban	12%	16%
Barelands/Fields	7%	11%
Forest/Vegetation	73%	69%

Figure 17. LCLU Classification, Spring Image 1990103--April 13, 1990

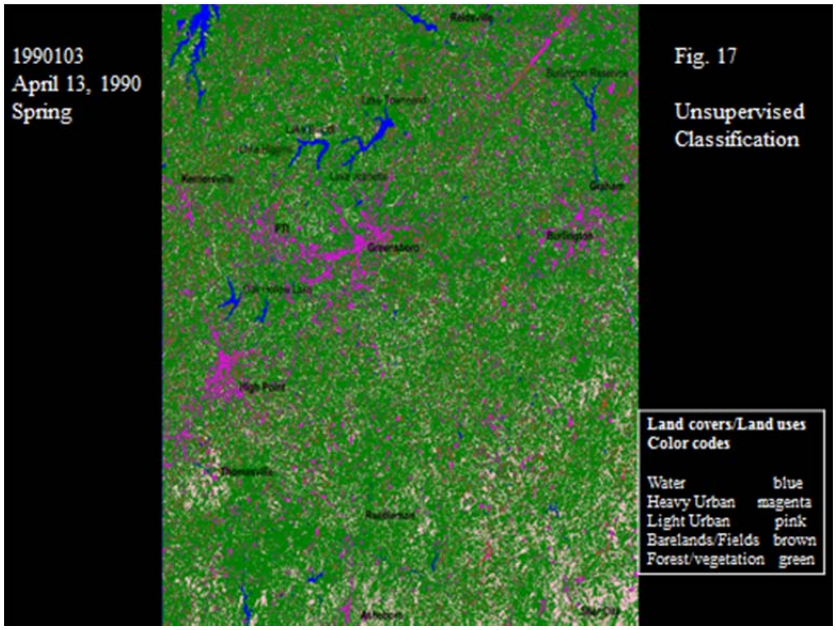

Figure 18. LCLU Classification, Spring Image 2000147--May 26, 2000

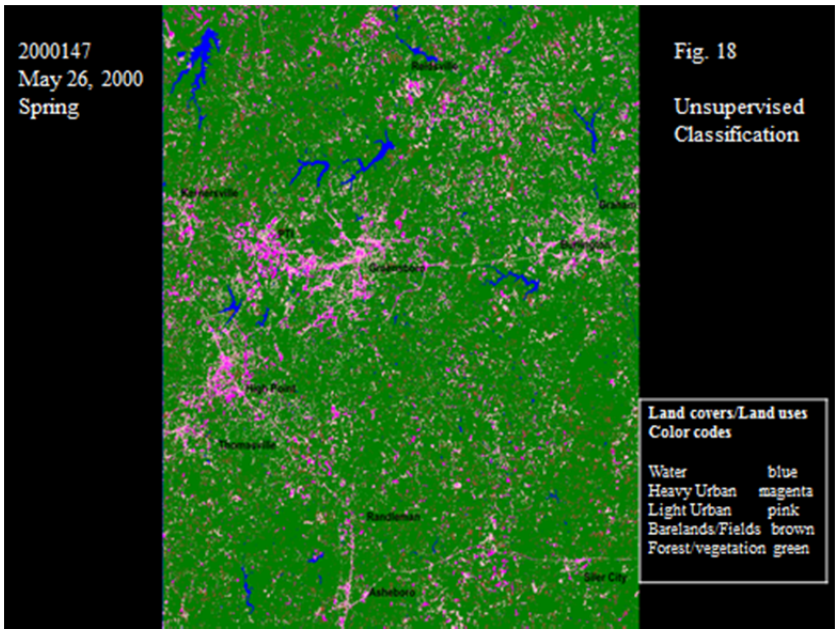

Table 18. Unsupervised Classification Percentages, Winter Seasons

Winter		
	Dec. 1990	Feb. 2000
Water	3%	1%
Heavy Urban	6%	5%
Light Urban	6%	11%
Barelands/Fields	5%	6%
Forest/Vegetation	80%	77%

Figure. 19. LCLU Classification, Winter Image 1990343--December 19, 1990

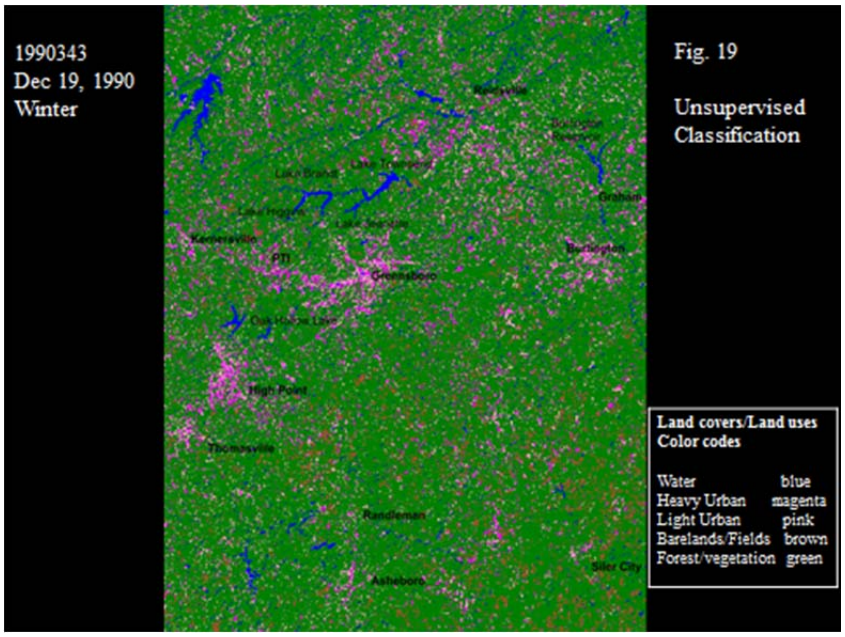

Figure. 20. LCLU Classification, Winter Image 200051--February 6, 2000

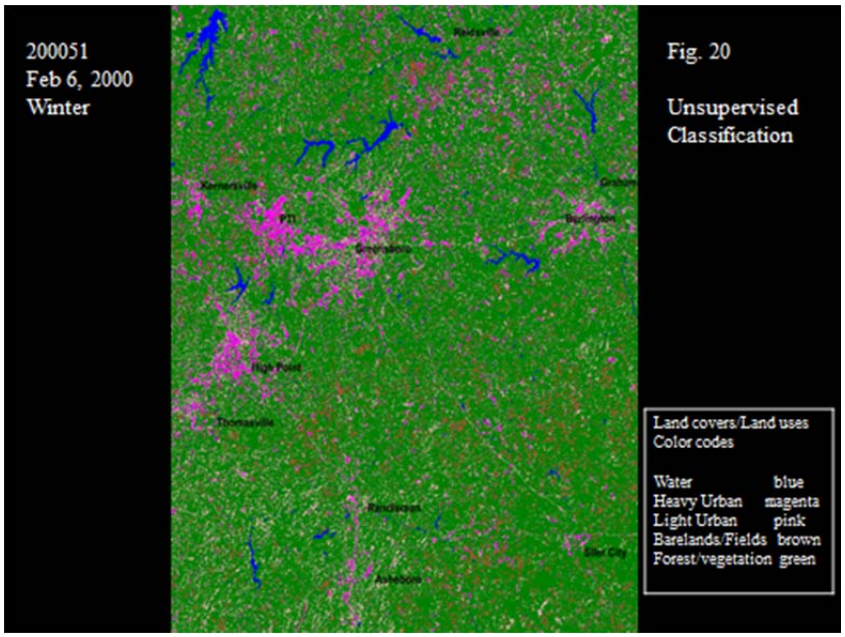

Compared, then, with the 1990 classifications, the 2000 forest/vegetation land covers generally had higher percentages. Water cover percentages were about the same on all the images, with the 2000 classifications being slightly higher. The combined urban land uses for the 2000 images had percentages similar to the 1990 images, except for the 2002 images, which showed much higher percentages. The 2002 spring image had the highest percentage of heavy/light urban land use among all the images (28%); however, moderate cloud cover causes a mixed pixel situation between the land uses.

One interesting analogy is that the barelands/fields land cover percentages varied little from year to year and season to season. Generally, the 1990 percentages were a little higher than the 2000 percentages. The corridor cities also have substantial commercial and residential development from 1990 to 2002 along with extensive highway construction. These results indicate that the spectral properties of these land use/land cover types in the corridor study area changes from year to year and season to season, but are more dramatic during the 2000's years, especially among the light/urban land uses.

The results also correlates with historical data (Google Earth, 2012) of the corridor study area and various accuracy assessment tasks were performed on the classes (classification overlay, error matrix, and accuracy totals reports), which gave sufficient results (overlays lined up correctly, high percentages according to accuracy totals report). Also, the 1992 images have greater percentages of light/heavy urban buildup than the 1990 and 1991 images in all seasons. This means residential /commercial development and road construction began to increase after 1990, which increased impervious surfaces that contributes to the development of surface urban heat islands.

The 2000 and 2002 summer seasons have the greatest percentages of total urban buildup (16% vs. 18%) respectively over the 1990 image (8%). The 2000 autumn season also has the greatest increase of total urban buildup (22%) over the 1990 image (13%). The spring images didn't show much variation or increases from 1990 to 2000, however, light urban growth (residential development) increased 4% from 1990 to 2000. Total urban land use buildup gradually increased from 1990 to 2002, which brought more impervious surfaces to the study area---bypass construction, more road networks, and commercial/residential buildup in various areas of the corridor cities and periphery areas. This supports Weng's results (Indianapolis, Indiana-2008) that impervious surfaces not only indicates the degree of urbanization, but is also a major contributor to the environmental impacts of urbanization.

The areal extent and spatial occurrence of impervious surfaces significantly influences urban climate by altering sensible and latent heat fluxes within the urban canopy and boundary layers. It can also be concluded that the spring, summer, and autumn classification images showed more texture and spatiality in the five land cover/ land uses than in the winter images. This means that the signatures from these land covers in those seasonal images contains more variation in spectral radiance than the winter images, which influences the spatial patterns of land use and land covers, helping to create thermal climates.

The unsupervised classification technique is a useful method in displaying the signature contrasts and spatiality of the five land cover/land use classes. The technique revealed urban and rural surface characteristics and broad urban coverage of the study

area, providing reliable and significant results that helped in observing and analyzing the UHI patterns in the I-85/I-40 corridor.

3.0. Normalized Difference Vegetation Index

NDVI values were calculated for displaying vegetation and non-vegetation/impervious surface density and assigning emissivity values to the selected five land cover/land use types. NDVI maps were prepared for each selected year for autumn, summer and spring, allowing comparisons between seasons and years. These maps were assigned 5 classes (same as the classification map scheme) to show the contrasts and differences between the vegetative density/non-vegetative density and soil characteristics of the five land cover/land use types from each image scene. The NDVI values of the five classes (water, heavy urban, light urban, barelands/fields, and forest/vegetation) ranges from -1 to 1; class ranges are shown in Table 18. The NDVI values for forest/vegetation land cover correlates with the NDVI Threshold Method algorithm (NDVI < 0.2; NDVI > 0.5; 0.2 <NDVI <0.5 = NDVI value range) which was applied in this study, however, the barelands/fields land cover and light urban land use had slightly higher values than the Threshold Method (NDVI <0.2).

As with the LCLU imagery produced for comparison, the majority of image pairs highlighted similar findings. Because of these similarities, image pairs from 1990 and 2000 were once again chosen to highlight findings here. From 1990 to 2000, for instance, the autumn images (Figures 20 and 21) indicated that the combination of heavy and light urban classes increased from 11 to 24 percent (Table 19). Barelands/fields and water, on the other hand, remained fairly stable. Forest/vegetation land cover decreased markedly.

Table 19. NDVI Classification Percentages, Autumn Seasons

Autumn						
	Oct. 1990			Nov. 2000		
	NDVI Range	Percent	Acres	NDVI Range	Percent	Acres
Water	-0.8 to -0.46	1%	12,731	-0.47 to - 0.09	1%	10,372
Heavy Urban	-0.06 to 0.3	3%	53,183	-0.13 to 0.1	3%	57,548
Light Urban	0.1 to 0.4	8%	129,246	0.1 to 0.3	21%	343,344
Barelands/ Fields	0.2 to 0.5	28%	470,312	0.25 to 0.4	29%	490,547
Forest/ Vegetation	0.3 to 0.7	60%	1,006,890	0.3 to 0.7	46%	769,187

Table 20. NDVI Classification Percentages, Summer Seasons

Summer						
	Aug. 1990			Aug. 2000		
	NDVI Range	Percent	Acres	NDVI Range	Percent	Acres
Water	-0.08 to 0.008	1%	4,739	-0.2 to -0.09	1%	7,187
Heavy Urban	0.009 to 0.3	3%	24,755	-0.09 to 0.16	2%	41,252
Light Urban	0.12 to 0.38	6%	93,137	0.16 to 0.42	10%	164,027
Barelands/ Fields	0.3 to 0.47	19%	317,533	0.37 to 0.52	16%	277,375
Forest/ Vegetation	0.4 to 0.68	72%	1,235,078	0.48 to 0.78	71%	1,182,123

Figure 21. 1990279 October 6, 1990--Autumn--945am DST

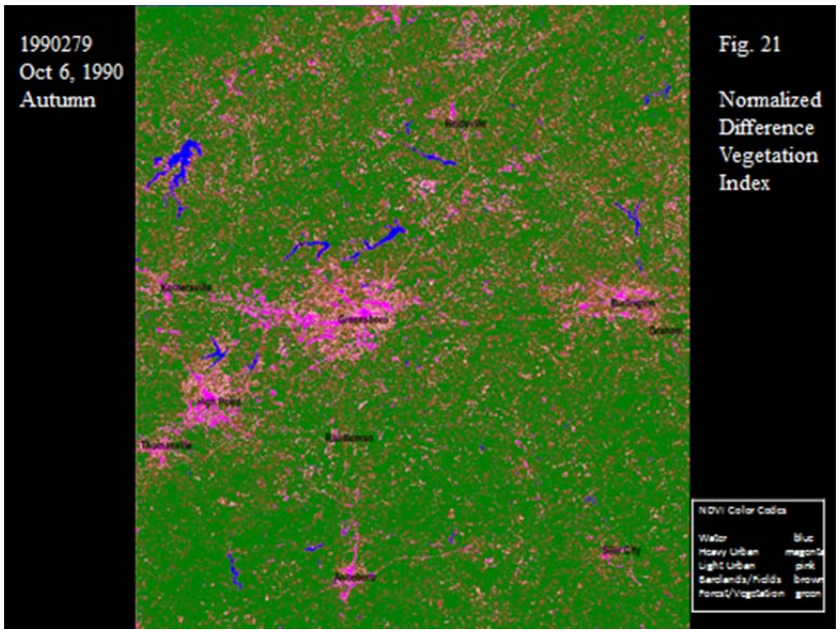

Figure 22. 2000307 November 1, 2000--Autumn--945am DST

Class ranges for the summer 1990 and NDVI images are similar to those for the autumn images (Table 18). Likewise, there was an increase in the combined urban landuse classes, growing from 9% in 1990 to 12% in 2000 (Figures 23 and 24). This pair of images also highlights the decrease in forest/vegetation land cover. The barelands/fields land cover again remained stable over the two intervals.

The spring 1990 and 2000 NDVI images (Table 21) show increases in heavy urban land cover and barelands/fields. Light urban areas appeared fairly stable across these two images, as did forest/vegetation (Figures 25 and 26). As this presents a somewhat different picture compared to the autumn and summer images, the 1990 spring image was also compared to the 2002 spring image (Figure 27). Findings were similar for the heavy and light urban land covers. Forest/vegetation showed an increase, however, from 58% to 63%.

Table 21. NDVI Classification Percentages, Spring Seasons

Spring						
	Apr. 1990			May 2000		
	NDVI Range	Percent	Acres	NDVI Range	Percent	Acres
Water	-0.02 to 0.45	1%	10,046	-0.06 to 0.5	1%	8963
Heavy Urban	0.1 to 0.13	1%	39,625	0.06 to 0.06	4%	62673
Light Urban	0.1 to 0.4	14%	226,642	0.07 to 0.4	12%	206875
Barelands/ Fields	0.3 to 0.6	26%	433,158	0.2 to 0.6	30%	499213
Forest/ Vegetation	0.4 to 0.8	58%	961,728	0.27 to 0.78	54%	894862

Figure 23. 1990215 August 3, 1990--Summer--945am DST

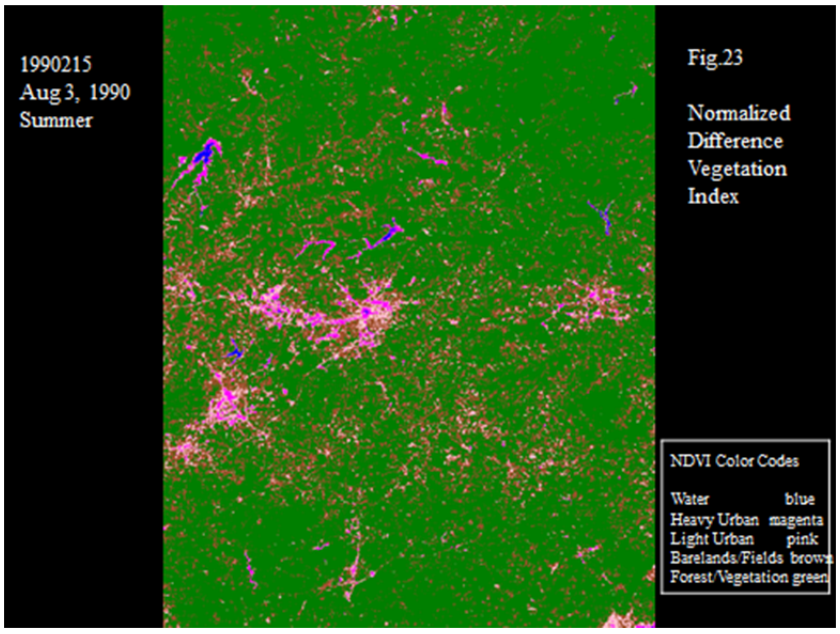

Figure 24. 2000227 August 14, 2000--Summer--945am DST

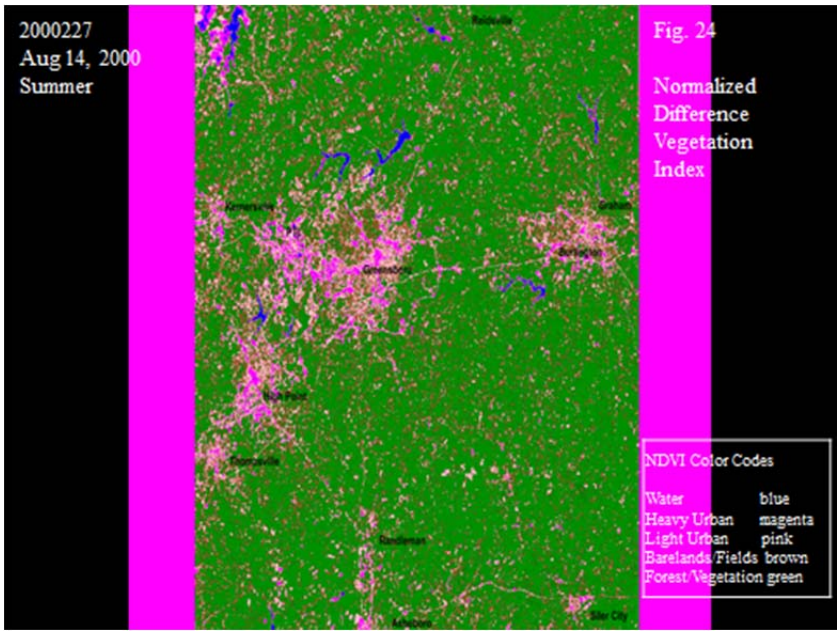

Figure 25. 1990103 April 13, 1990--Spring--945am DST

Figure. 26. 2000147 May 26, 2000--Spring--945am DST

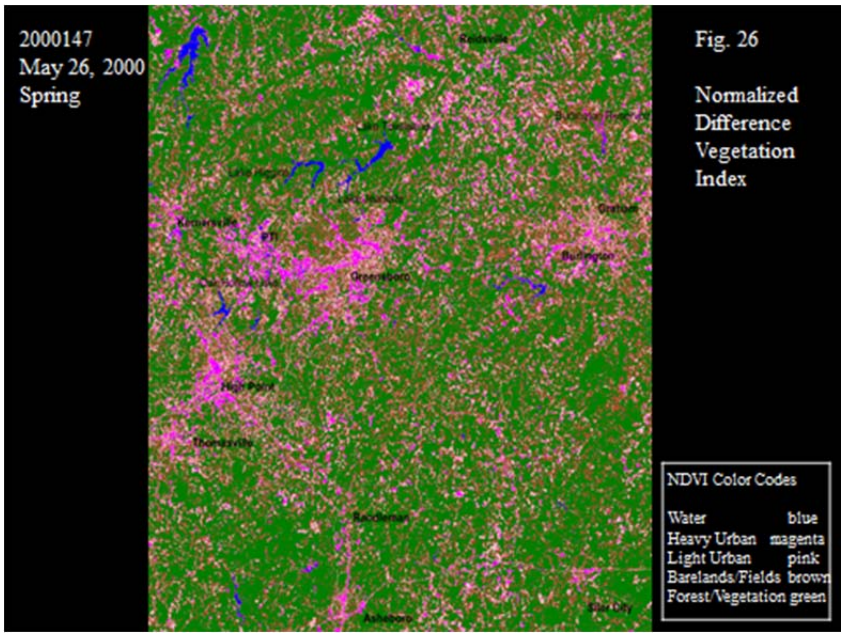

Figure. 27. 2002168 June 17, 2002--Spring--945am DST

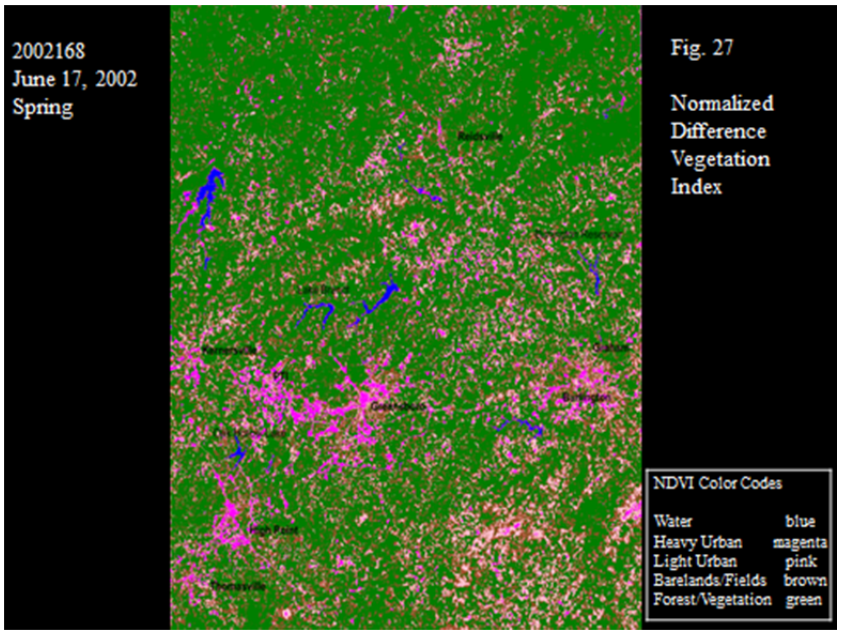

In summary, the forest/vegetation land cover for all the NDVI images appears to correlate with Sobrino's NDVI Threshold Methods algorithm (NDVI >5) with an assigned emissivity value of .99. Also, the algorithm's mixed pixel range between 0.2 and 0.5 was similar to the images' barelands/fields and forest/vegetation land covers. The algorithm indicates NDVI values greater than 0.5 were fully vegetated and forested. NDVI values between 0.2 and 0.5 indicates mixed pixels of bare soil and vegetation and NDVI values between 0 and .2 represented the barelands/fields, light/heavy urban land covers and water areas with assigned emissivity values around .97, .96 and .99 respectively. The majority of the negative NDVI values (NDVI < 0), as would be expected, occurred in the heavy urban land uses and all water areas. The study region's barelands/fields land cover and light/heavy urban land uses had slightly higher NDVI values, which slightly increased the emissivity values.

Topography and land cover differentiation is a major factor because Sobrino's NDVI Threshold Methods algorithm was originally applied to an agricultural region in Spain while the I-85/I-40 corridor is more forested and urbanized, hence the higher values. This also indicates the emissivity values are slightly adjusted for the study area: forest/vegetation and water--0.99; barelands/fields— 0.98; and light/heavy urban land cover--96 to 97. These results suggest dramatic urbanization was occurring between the time intervals, while the barelands/fields land cover generally decreased. This is supportive of the fact that urbanization has increased in the region between the two intervals with reductions in barelands/fields land covers.

The combined urban land covers were more extensive in the 2000 summer and autumn images than the 1990 spring and summer images. These results suggest that the seasonal NDVI images, especially autumn and summer, show how urbanization has increased between the two intervals. The contrast between vegetation and urban areas, however, were not as apparent in the winter NDVI images. Thus, the UHI effect seems to occur more during the summer thru the autumn seasons which correlates with Oke (1982) UHI characteristics. Indicating their large variation, the highest average values of NDVI occurred in the spring (mean=0.7629) and summer (mean=0.7155) seasons among all the dates. The autumn seasons had moderate high values with a mean of (0.6933) indicating a foliage decrease (green reduction) from July to October while winter seasons had the smaller ranges with a mean of (0.6292) and lower values. Higher values of NDVI usually indicate a larger fraction of vegetation in a pixel and lower values indicate a larger fraction of impervious and water surfaces. Also, the 2000 images in the autumn, spring, and summer seasons had higher mean NDVI values than the 1990 seasonal images.

The 1990 autumn, summer, and spring scenes have the widest NDVI values for total urban land use, with summer having the widest (-0.06 to .40). The 2000 autumn, summer, and spring scenes also have the widest NDVI values for total urban land use, with summer having the widest (-0.06 to .42). What is interesting is that both intervals have similar wide NDVI values for the summer. Compared to the 1990 interval, the results revealed from the range of NDVI values regarding the 2000 light/heavy urban land use also have wider ranges during the summer and autumn than the spring and winter. This is an indication that the 2000 interval not only has more total urban buildup

than 1990, but also that the urban heat island climates are more prevalent during the 2000 interval. Also, the wider ranges of NDVI values represents more pixels for that particular class, which as for the case of total urban land use, means more residential/commercial development and highway construction.

Oke (1982) argues that the UHI is strongest in the late summer and fall seasons, and this study's results seems to correlate with Oke's argument. The 2000 spring and summer images shows substantial increases in LST's when compared with the 1990 spring and summer images at all locations (weather stations and the 15 selected locations) while the 1990 and 2000 autumn and winter images had no definite LST temperature pattern when compared against one another. However, in all the 1990 and 2000 images, the water areas (Lakes Brandt and Oak Hollow Lake) and the rural locations of Sedalia and Randleman always had the lowest LST temperatures. It appears that all the hourly minimum temperatures and the satellite land surface temperatures have somewhat similar temperatures that is quite evident in all the seasons of the 2000 interval.

On the basis of these comparisons, it appears that the NDVI technique, when matched with land cover classifications, shows some promise for detecting how the vegetation density/non vegetation density signatures of the five land cover/land use types influence the regional temperature rise in the study area. This technique also revealed more dramatic contrasts between the urban and rural land covers and uses. Impervious surfaces (urbanization) appear to be a major contributor to regional temperature rise in the I/85/I-40 corridor area during the spring, summer and early autumn seasons. Results

also suggested that the impact of land use/land cover spatiality on temperature rise occurred dramatically from 1990 to 2002.

4.0. Statistical Analysis Results

To explore the relationship between NDVI values and LSTs further, scatterplots of the relationship between the two, shown over the four seasons, are graphed in Figure 27. For NDVI values to be strong predictors of the UHI effect, a strong linear relationship should be present when the values are graphed in the scatterplot. In this study, despite the comparative relationships noted between NDVI values and land cover classes, the relationships between NDVI and LST values appear to be more nonlinear; they also seem to be influenced by the individual season. For example, the most linear of the scatterplots appears to be the one for summer, suggesting that it may be possible to use NDVI values as a means of analyzing UHI effects in the study area for this particular season. Although the relationship does not appear as strong, it is also possible to discern a linear relationship in the spring scatterplot.

Figure 28. Scatterplots showing the relationships between LSTs and NDVIs

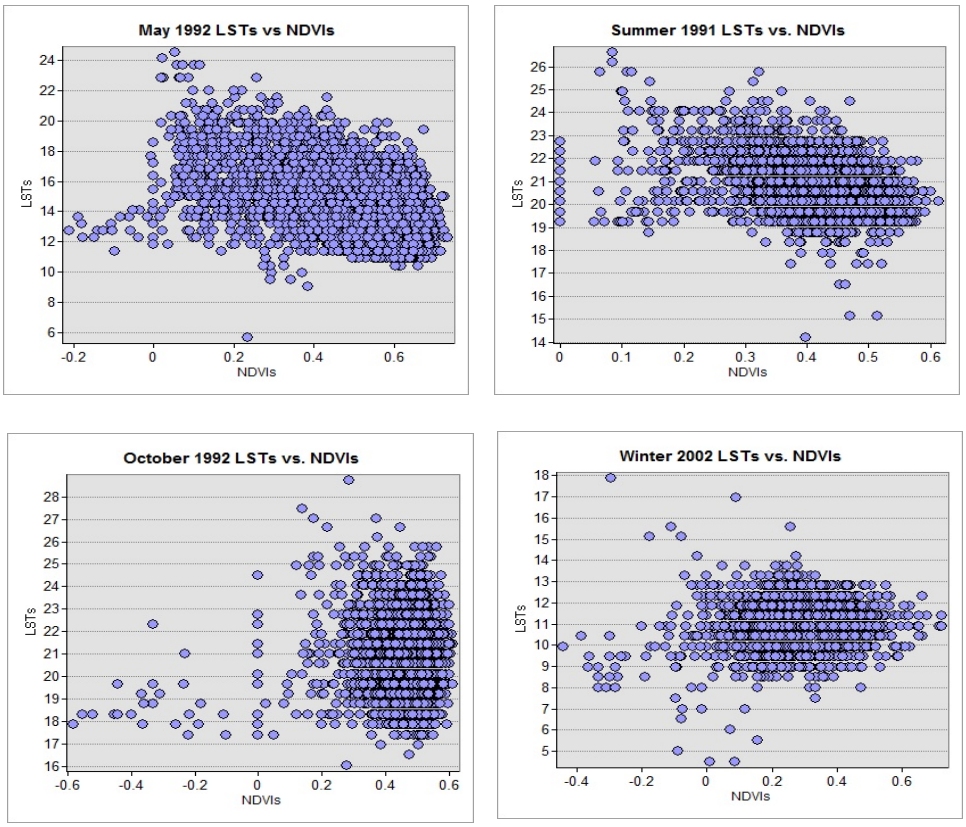

These possible relationships were also examined using a zonal analysis, in which mean LST values were plotted against small increments of NDVI values for each season. Trend lines were then overlaid to assess the relationship between LSTs and NDVIs in more detail. As Figure 28 shows, the relationship between mean LST values and NDVI values for the spring and summer images are complex and generally unstable. However, there is a noticeable inverse trend between LSTs and higher NDVI values, as would be expected for NDVIs to be useful in analyzing UHI effects. The relationship between mean LST values and NDVI values for fall and winter do not indicate the expected inverse trend between values, but instead suggest a more positive trend, where increased

LSTs are associated with higher NDVI values. These higher NDVI values are not useful in predicting LST values for the autumn and winter seasons. This occurs because of the foliage decrease in these seasons. Also, higher average NDVI values occurred in the spring and summer (page 60) due to generally high foliage cover over the autumn and winter seasons. The spring and summer seasons also exhibited higher urban activity with increased anthropogenic heat sources than the autumn and winter seasons.

Figure 29. Results of zonal analysis, comparing mean LSTs against classified NDVI Ranges

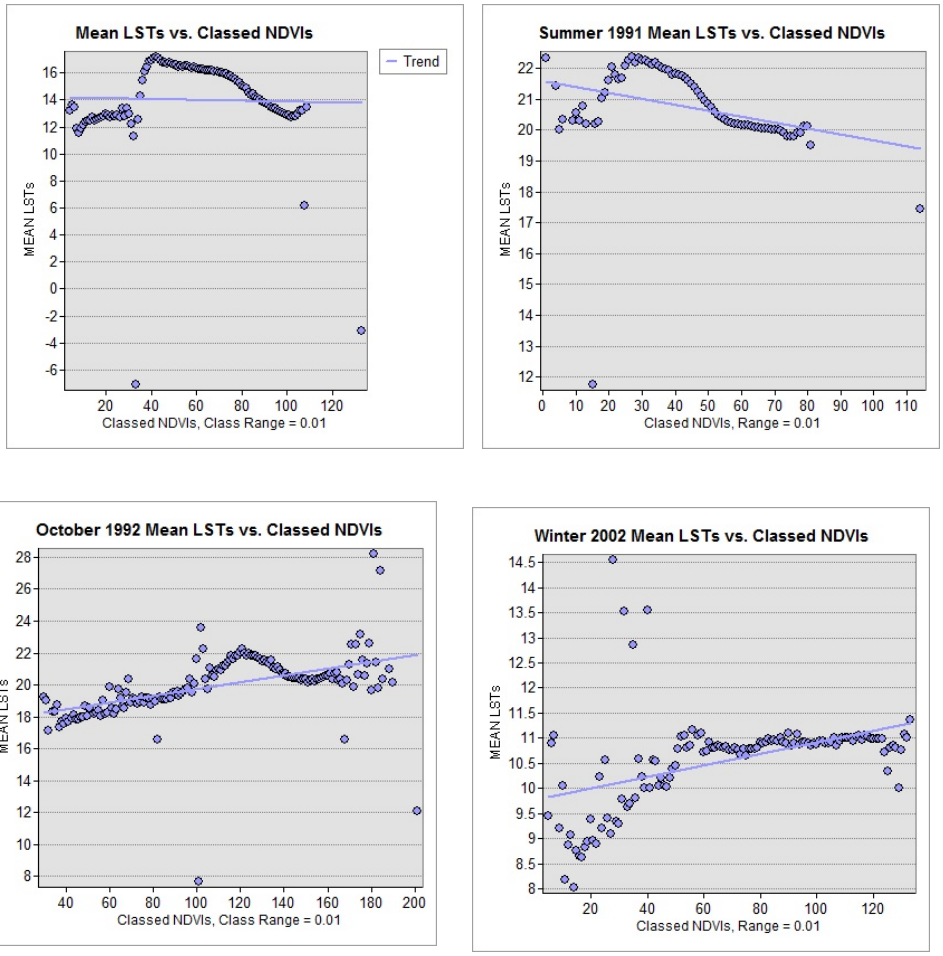

CHAPTER V

CONCLUSION

This study has demonstrated that urban heat island climates exist in the urban centers and some surrounding areas in the study area. The three largest cities—Greensboro, High Point, and Burlington—all have heat islands located in various parts of their community. The I-85/Bus 85 split also had heat island activity, as did areas around PTI airport. These heat islands have grown from the 1990s to the 2000s and their spatial extent is getting larger as the study area continues to grow, especially in the larger urban centers.

The unsupervised classification maps displayed the five landcover/land uses clearly and was able to distinguish the spatiality between each one. The spectral signatures not only revealed the heterogeneity of the land cover types and land uses, but how they have changed from the 1990s to the 2000s. The NDVI images seemed to correlate well, showing how the vegetation and non- vegetation signatures of the various land cover types/land uses have changed with the seasons along with greater spatial extent especially during the 2000s spring and summer seasons.

Land use/land cover changes, especially urban development, can alter the patterns and development of UHI's and the patterns of land cover in this study indicated this in the unsupervised classification and the NDVI maps of the corridor area. However, results also showed that NDVI values alone are not effective in representing urban area

thermal properties (Xian & Crane, 2006). A combination, however, of NDVI, Unsupervised Classifications, and LST's seem to describe the spatial distribution and temporal variation in urban thermal patterns and associated LULC conditions better. The LST maps showed the spatial extent of the urban heat islands and how they have grown and changed, especially doing the spring and summer months. The cooler spots in all the selected LST images were consistently the rural areas such as Randleman and Sedalia along with all the water areas (city lakes, etc). The LST maps also highlighted the "hot spots" in the study area, especially in the urban areas, PTI airport periphery, and the I-85/ Business 85 split. These "hot spots" represents probable heat islands and significant thermal climate activity. This means that regional temperature rise seems to be contributable to thermal climates or UHI development in various locations throughout the corridor area.

Remote sensing techniques worked well for analyzing UHI development, however, it was difficult to select images with similar conditions of atmosphere, hydrology, and landcover/land use areas (Chen et al., 2005). Nevertheless, the applications were useful for characterizing urban and rural landscape patterns and for analyzing land surface temperatures and urban heat island climates. This study supported and confirmed Lee's (1992) concepts that remote sensing techniques will generate reliable results by analyzing and interpreting temperature data. Digital remote sensing technology provided not only a measure of the spatial extent of land surface temperatures of the entire corridor, but allowed the texture and behavior of these surface heat island climates to be observed and analyzed. The study results also demonstrated the

capabilities of remote sensing applications to derive some components of the urban energy balance and to monitor their spatial and temporal variability.

The application of satellite sensors to determine brightness and radiometric temperature is complicated by any heterogeneity or roughness of the land, therefore, this becomes a significant issue when dealing with urban surfaces. Improving the interpretation of urban surfaces will require better parameters to overcome the difficulties of making observations over the relatively tall urban surface compared to the shorter vegetated surfaces. The study area has smooth topography and moderate land cover heterogeneity, which helps in determining brightness and radiometric temperatures in this case. The sun–synchronous orbit characteristic of Landsat satellites are not ideal for dynamic surface heat island analysis, nevertheless, the temperature data provided useful information for measuring and understanding urban heat island effects.

Remote sensing applications should continue to be used to refine and estimate appropriate parameters to describe the urban surface; these can then be applied to urban climate models. As remotely sensed data extend to include high resolution data, satellite based urban climate studies will become more feasible not only in studying large-scale UHI characteristics but also in exploring meso-scale urban meteorology. Future studies for improvement of results for the corridor study area should involve (1) adding more hourly daily minimum temperature data from more weather stations in the area; (2) increasing the study area extent, maybe all of central North Carolina instead of the Piedmont Triad periphery; (3) integrating both unsupervised and supervised classifications to get better results showing land cover/land use signatures; (4)using

higher spectral and spatial resolution of satellite data (ASTER, etc) to increase the definition of the land covers and land uses resulting in better interpretation of the area; (5) constructing maps of physical surface properties such as albedo and emissivity and employing layers of air quality information; (6) including additional hourly temperature data to improve sample sizes for statistical operations; (7) improving methods of land surface temperature retrieval to reduce the influence of thin cloud atmospheric conditions; and (8) using multiple regression, kriging, and other geostatistical applications to examine how such techniques might modify this study's results.

Advancement of the qualitative description of thermal patterns, along with basic correlation studies requires more fundamental surface descriptors than using qualitatively based land use data to describe the urban surface (Voogt & Oke, 2003). The results of this study contributes "cutting edge" knowledge and information about urban thermal climates to academia, local, state, and federal governments, developers , environmental interest groups and other stakeholders. This will increase better awareness and understanding on how to control, manage, and mitigate these thermal climates for a healthier and sustainable urban and rural environment for the I-85/I-40 corridor study area.

REFERENCES

Ahmad, A. & Hashim, N. (2007). A remote sensing-GIS evaluation of urban growth-land surface temperature relationships in Selangor, Malaysia. Retrieved Nov 28, 2007 from http//www.GISdevelopment.net

Aniello, C., Morgan, K., Busbey, A., & Newland, L. (1995). Mapping micro-urban heat islands using Landsat TM and a GIS. *Computers and Geosciences*, 21, 965-969

Carlson, T.N., Augustine, J.A., & Boland, F.E. (1977)**.** Potential application of satellite temperature measurements in the analysis of land use over urban areas. *Bulletin of American Meteorological Society, 58,* 1301-1303.

Camilloni, I., & Barros, V. (1997). On the urban heat island effect dependence on temperature trends. *Climate Change, 37,* 665-681.

Changon, S.A. (1992). Inadvertent weather modification in urban areas: lessons for global climate change. *Bulletin of the American Meteorological Society, 73,* 621-627.

Chen, X.L., Zhao, H., Li, P. & Yin, Z. (2006). Remote Sensing image-based analysis of the relationship between urban heat island and land use/cover change. *Remote Sensing of Environment*, 104, 133-140

Congalton, R.G. (1991)**.** A review of assessing the accuracy of classifications of remotely-sensed data. *Remote Sensing of Environment*, 37, 35-46

Dousset, B., & Gourmelon, F. (2003). Satellite multi-sensor data analysis of urban surface temperatures and land cover. *ISPRS Journal of Photogrammetry and Remote Sensing, 58,* 43-64.

Florio, E. N., Lele, S.R., Chung, Y. C., Sterner, R., & Glass, G.E. (2004). Intergrating AVHRR satellite data and NOAA ground observations to predict surface temperatures: a statistical approach. *International Journal of Remote Sensing, 10,* 2979-2994.

Gallo, K.P., McNab, A.L., Karl, T.R., Brown, J.F., Tarpley, J.D. & Hood, J.J. (1993). The use of NOAA AVHRR data for assessment of the UHI Effect. *Journal of Applied Meteorology, 32,* 899-908.

Gallo, K.P., & Owen, T. W. (1999). Satellite-based adjustments for the urban heat island temperature bias. *Journal of Applied Meteorology, 38,* 806-813.

Gallo, K.P., Tarpley, J.D., McNab, A.L., & Karl, T.R. (1994). Assessment of urban heat islands: A satellite perspective. *Atmospheric Research, 37,* 37-43.

Gluch, R., Quattrochi, D.A.,& Luvall, J.C. (2006). A multi scale approach to urban thermal analysis. *Remote Sensing of Environment, 104,* 123-132.

Google Earth (2012) United States Geological Survey.{ Web Link} Accessed 6/25/12

Henry, J.A., Dicks, S.E., Wetterqvist, O.F., & Roguski, S.J. (1989). Comparison of satellite ground-based, and modeling techniques for analyzing the urban heat island. *Photographic Engineering of Remote Sensing, 55,* 69-76.

Hung, T., Uchihama, D., Ochi, S. & Yasuoka, Y. (2006). Assessment with satellite data of the urban heat island effects in Asian mega cities. *International Journal of Applied Earth Observation and Geo information, 8,* 34-48.

Jensen, J.R. (2005) Introductory Digital Image Processing: New Jersey:Prentice Hall

Landsberg, H. E. (1981) *The urban climate*. New York: Academic Press.

Lee, H. (1993). An application of NOAA AVHRR thermal data to the study of urban heat islands. *Atmospheric Environment, 27B,* 1-13.

Li, F., Jackson, T.J., Kustas, W..P., Schmugge, T. J., French, A. N., Cosh, M. H., & Bindlish, R. (2004). Deriving land surface temperature from Landsat 5 and 7 during SMEX02/SMACEX. Remote Sensing of Environment, 92, 521-534

Li, J., Wang, X R.., Wang, X J., Ma, W., & Zhang, H. (2009). Remote sensing evaluation of urban heat island and its spatial pattern of the Shanghai metropolitan area, China. *Ecological Complexity*, 30, 1-8

Lo, C.P., & Quattrochi, D.A. (1997). Application of high resolution thermal infrared remote sensing and GIS to access the urban heat island effect. *International Journal of Remote Sensing, 18,* 287-304

Memon, R.A., Leung, D.Y.C., Liu, Chun-Ho. (2009) An investigation of urban heat island intensity (UHII) as an indicator of urban heating. *Atmospheric Research,* 94, 491-500

National Climatic Data Center (2012) NCDC Map Services. {Web Database} Available: http: //www.ncdc.noaa.gov. Accessed 5/17/12

Nichol, J.E. (1996). Visualization of urban surface temperatures derived from satellite images. *International Journal of Remote Sensing, 19*, 1639-1649.

Oke, T.R. (1982). The energetic basis of the urban heat island. *Quarterly Journal of Royal Meteorological Society, 108,* 1-24.

Oke, T.R. (1987) *Boundary layer climates*. New York: Methuen Press

Owen, T.W., Carlson, T.N., & Gillies, R.R. (1998). An assessment of satellite remotely sensed land cover parameters in quantitatively describing the climatic effect of urbanization. *International Journal of Remote Sensing, 19*, 1663-1681.

Quattrochi, D. A., & Luvall, J.C. (1997). Application of high resolution thermal infrared remote sensing and GIS to assess the urban heat island effect. *International Journal of Remote Sensing, 18*, 287-304.

Rao, P.K. (1972). Remote Sensing of urban heat islands from an environmental satellite. *Bulletin of American Meteorological Society*, 53, 647-648.

Rigo, G., Parlow, E., & Oesch, D. (2006). Validation of satellite observed thermal emission with in situ measurements over and urban surface. *Remote Sensing of Environment, 104*, 201-210.

Rosenzweig, C., Solecki, W.D., Paschall, L., Chopping, M., Pope, G., & Goldberg, R. (2005). Characterizing the urban heat island in current and future climates New Jersey. *Environmental Hazards, 6*, 51-62.

Roth, M., & Oke, T.R. (1989). Satellite derived urban heat islands from three coastal cities and the utilization of such data in urban climatology. *International Journal of Remote Sensing, 10*, 1699-1720.

Sobrino, J. A., Jimenez-Munoz, J. C., & Paolini, L. (2004). Land surface temperature retrieval from Landsat TM 5. *Remote Sensing of Environment*, 90, 434-440

Southeast Regional Climate Center (2009). Climate Interactive Rapid Retrieval User System. {Web Database} Available: http//www.dnr/statesc/pls/cirrus/cirrus. Accessed: 3/18/09

State Climate Office of North Carolina (SCONC) (2009). Climate Normals/Stations/ Summaries/Data Request Forms. {Web Database} Available: http//www.nc-climate.ncsu.edu. Accessed: 4/23/09

Stathopoulou, M., Cartalis, C, & Kermatisoglou, I. (2004). Mapping micro urban heat islands using NOAA/AVHRR images and CORINE land cover: an application to coastal cities of Greece. *International Journal of Remote Sensing, 25*, 2301-2316.

Stathopoulou, M. & Cartalis, C. (2007). Daytime urban heat islands from Landsat ETM+ and Corine land cover data: An application to major cities in Greece. *Solar Energy*, 81, 358-368

Streutker, D.R. (2003). Satellite measured growth of the urban heat island of Houston, Texas. *Remote Sensing of Environment, 85*, 282-289.

Streutker, D.R. (2003). A remote sensing study of the urban heat island of Houston, Texas. *International Journal of Remote Sensing, 23*, 2595-2608.

United States Bureau of the Census. (2001, 2005). Census of Population: 2000 Vol. 2, Characteristics of the Population, Part 43, North Carolina, Washington, D.C: Government Printing Office.

United States Geological Survey (USGS) (2008). Satellite Division: Earth Science Resource Observation Systems Data Center—Earth Explorer. {Web database} Available: http//www.usgs.gov. Accessed 8/1/08

Voogt, J.A., & Oke, T.R. (2003). Thermal remote sensing of urban climates. *Remote Sensing of the Environment*, 86, 370-384

Weng, Q. (2009). Thermal infrared remote sensing for urban climate and environmental studies: Methods, applications, and trends. *International Journal of Remote Sensing*, 64, 335-344

Weng, Q., & Lu, D. (2008). A sub-pixel analysis of urbanization effect on land surface temperature and its interplay with impervious surface and vegetation coverage in Indianapolis, Untied States. *International Journal of Applied Earth Observation and Geoinformation*, 10, 68-83

Xian, G. & Crane, M. (2006). An analysis of urban thermal characteristics and associated land cover in Tampa Bay and Las Vegas using Landsat satellite data. *Remote Sensing of Environment*, 104, 147-145

Xiao, R., Ouyang, Z., Zheng, H., Li, W., Schienke, E. W., & Wang, X. (2006). Spatial pattern of impervious surfaces and their impacts on land surface temperature in Beijing, China. *Journal of Environmental Sciences*, 19, 250-256

Yagoub, M.M. (2004). Monitoring of urban growth of a desert city through remote sensing: Al-Ain, UAE, between 1976-2000. *International Journal of Remote Sensing, 25*, 1063-1076.

Yang, J., & Wang, Y.Q. (2007). Estimation of land surface temperature using Landsat-7 EMT thermal infrared and weather station data. Department of Natural Resource Sciences, 1

Yuan, F., & Bauer, M. E. (2007). Comparison of impervious surface area and normalized difference vegetation index as indicators of surface urban heat island effects in Landsat imagery. *Remote Sensing of Environment*, 106, 375-386

Zhang, J., Wang, Y., & Li, Y. (2006). A C + program for retrieving land surface temperature from the data of Landsat TM/ETM + band6. *Computers and Geosciences*, 32, 1796-1805